CESIUM-133 NUCLEAR MAGNETIC RESONANCE STUDY OF CESIUM SALTS AND COMPLEXES IN NON-AQUEOUS SOLVENTS

Thesis for the Degree of M. S.
MICHIGAN STATE UNIVERSITY
LULU LIU HSU
1976

ABSTRACT

CESIUM-133 NUCLEAR MAGNETIC RESONANCE STUDY OF CESIUM SALTS AND COMPLEXES IN NON-AQUEOUS SOLVENTS

By

Lulu Liu Hsu

Non-proton NMR has been established as an important technique for the the study of chemical systems in solution. In particular, alkali metal NMR has been widely used in the investigation of solution interactions. ^{133}Cs NMR has been little employed until recently. However, with the advances in fourier transform NMR instrumentation, it is now readily available.

^{133}Cs NMR has been used previously by DeWitte (see Ref. 27) to study one-to-one electrolytes in different solvents. An attempt was made to correlate the chemical shifts of the infinitely dilute cesium ion in each solvent with the donor number established empirically by Gutmann. The discussion includes all the ^{133}Cs NMR data available from both studies. The effects of solvent and anion on the ion pair phenomenon are examined and association constants determined.

After Lehn first synthesized the macrobicycles, cryptands, considerable interest was generated as these ligands form unusually strong complexes with alkali metal ions. Besides their biological applications, these three-dimensional ligands have tremendous potential in chemical reaction. The topology and selectivity of these compounds can be used to advantage in the control and study of alkali metal interactions in solution. The C211, C221 and C222 cryptands are used in this study and the complexation interactions with the cesium ion are studied in various solvents. Temperature effects on the complexation reaction are also given.

CESIUM-133 NUCLEAR MAGNETIC RESONANCE STUDY OF CESIUM SALTS AND COMPLEXES IN NON-AQUEOUS SOLVENTS

By

Lulu Liu Hsu

A THESIS

Submitted to
Michigan State University
in partial fulfillment of the requirements
for the degree of

MASTER OF SCIENCE

Department of Chemistry

1976

ACKNOWLEDGEMENTS

The author wishes to thank Professor Alexander I. Popov for his guidance, counseling and encouragement throughout this study.

Financial aid from the Department of Chemistry, Michigan State University and the National Science Foundation is gratefully acknowledged. Appreciation is extended to Frank Bennis and Wayne Burkhardt for their help with the NMR spectrometer.

I would like to thank all the members of Dr. A. I. Popov's research group for the many enlightening discussions shared and the general feeling of friendship and goodwill. And to Ada and Spiros Hourdakis, special thanks for all the good times, both Greek and Chinese, that we shared.

TABLE OF CONTENTS

TABLE OF CONTENTS (Continued)

LIST OF TABLES

LIST OF FIGURES

LIST OF FIGURES (Continued)

LIST OF FIGURES (Continued)

CHAPTER I

HISTORICAL

NUCLEAR MAGNETIC RESONANCE STUDIES OF SOLVATION AND IONIC ASSOCIATION

Alkali metal NMR has grown tremendously in the past few years as an important analytical technique in the study of interactions in solutions. Such studies includes ion pair formation (1-5), complexation (6-10) and competitive interactions (11) in aqueous and non-aqueous solvents as well as mixed solvent work (12-14). In an NMR experiment, the experimental parameters one can follow are the chemical shift of the resonance, line width and relaxation time. These parameters can be monitored individually (5) or in concert (14).

In general, lithium-7 and sodium-23 NMR measurements have been often used since these two nuclei have sensitivities of 1.94 and 1.32 respectively, relative to an equal number of protons at constant frequency. Nuclear magnetic resonance studies of ^{39}K, ^{40}K and ^{41}K have been done by Sahm and Swenk (15) and other researchers (12,16) in aqueous and a few non-aqueous solutions. The rubidium-87 nucleus is less conducive to NMR studies due to its extremely broad line widths (17) though aqueous solutions have been investigated (16).

The nuclear magnetic resonance of the cesium-133 nucleus has not been investigated in any detail until this time. As early as 1953, Gutowsky and McGarvey (18) conducted a cesium-133 NMR experiment on solid state cesium halides and showed that the chemical shifts varied from one halide to another, which is indicative of some covalency in the supposedly "ionic bond". A later work by Bloemberg and Sorokin (19) determined the shielding constant, spin-lattice relaxation time

and isotropic exchange coupling for a single crystal of cesium bromide. An average of 25% covalency was deduced. The cesium chloride crystal structure was studied by monitoring the ^{133}Cs chemical shift, line width, lineshape and intensities in another study by Baron (20). This was followed by more works on cesium salts in solution (21-24), the most comprehensive of which are by Richards and co-workers (25,26) and DeWitte, et al. (27).

Other techniques commonly employed to study solvation and complexation in electrolyte solutions are conductance, solvent extraction, ultrasonic relaxation, ultra-violet, visible and infrared spectroscopy, far infrared spectroscopy, potentiometry and electron spin resonance.

In a simple one-to-one electrolyte solution, there are different kinds of interactions present. The type and magnitude of interaction are dependent on a number of factors, solvation number of the ions, solvating ability of the solvent, dielectric constant and structure making or breaking ability of the solute. Gutmann's donor number* is commonly used as a measure of the solvating ability of a given solvent (30).

The association of ions can be described by three models (at low concentrations): the contact ion pair, solvent shared ion pair and solvent separated ion pair (31). The contact ion pair is the classical

---

*The Gutmann donor number (28) is the enthalpy of complex formation between the given solvent and antimony pentachloride in 1,2-dichloroethane solution.

$$S + SbCl_5 \xrightarrow{1,2\text{-DCE}} S \cdot SbCl_5$$

The term "donicity" refers to the donor ability of a solvent. Gutmann recently introduced the concept of acceptor number of a solvent (29).

Bjerrium ion pair with a finite lifetime. Bloor and Kidd (2) noted varying degrees of concentration dependence of the ^{23}Na chemical shifts of the iodide salt and postulated contact interaction. Evans and Lo (32) observed vibrational bands which are neither solvent or salt vibrations and attributed them to the tetraalkylammonium cation and halide anion vibration. Balasubrahmanyam and Janz (33) studied silver nitrate solutions spectroscopically and observed two bands in the nitrate stretching frequency region and showed that they correspended to the free, solvated nitrate ion and the ion paired nitrate anion. The concentration dependence of the ^{19}F chemical shift observed by a number of investigators (34,35) was explained by the contact ion pair model.

The solvent shared and solvent separated ion pairs would be expected to occur in solutions where the electron donating ability of the solvent is much superior to that of the anion. Generally, if solvent-solute interaction is stronger than solute-solute interaction, ion pair formation would be limited. The extensive ^{23}Na NMR study conducted by Greenberg (36) with various solvents and salts showed that the tetraphenylborate salt is only weakly associated in solvents of low donicity and no ion pair formation was found in high donor solvents up to a concentration of 0.5 M. The iodide, thiocyanate and perchlorate salt solutions show more concentration dependence of the chemical shift. These results are supported by far infrared evidence of a solvent dependent and anion independent vibration band of the sodium ion (37).

A conductance study of alkali halides in various solvents by Kay (38) showed increasing ion pair association with increasing cation size (for lithium, sodium and potassium ions) in ethanol, 1-propanol and

liquid ammonia solutions. These results would seem to contradict the classical concept of the ion pair interaction, the strength of which is determined by the distance of closest approach of the two charge centers, which, in turn, is determined by the "ionic radii". Further work by Kay, et al. (39) showed that in anhydrous acetonitrile, except for cesium salts, alkali metal perchlorates are associated while the tetraphenylborate salts are completely dissociated. Minc and Werblem (40) also reported the same trend in ionic associations of the alkali metal perchlorates in acetonitrile. These results seem to indicate that, in the case of the smaller cations, solvation interaction is strong while the larger ion, cesium, appears to be much less solvated and ion pair formation, probably of the contact kind, can occur. Atlani and Justice (41) studied the conductimetric behavior of one-to-one electrolytes in dimethylsulfoxide and hexamethylphosphoramide and concluded that solvation effects on the tetraalkylammonium salts increase ion mobility and short range interactions between cations and anions. Potassium and sodium salts, if they associate at all, show contact ion pair formation. Further evidence for the importance of ion size in ion pair formation is given by Berman and Stengle (42) who used ^{35}Cl NMR line widths to show that contact ion pair formation is favored by high charge-to-size ratio of cation, low dielectric constant and low donor number for the perchlorate salts of sodium, lithium and magnesium. The extent of ionic association can be related to the dipole moment of the resulting ion pair. This effect was studied by Story and Hebert (43) by electric deflection experiments and they report an increase in electric dipole moment in the order KI < RbI < CsI.

Nuclear magnetic resonance studies have also been conducted using the anion as a probe (44-47). However, this approach is considerably more difficult. Anion solvation is less readily detected in solution as most solvents do not possess localized positive charges. Furthermore, the choice of anion is limited to those possessing nuclei that have easily accessible frequencies. Deverell and Richards (48) studied ^{35}Cl, ^{81}Br and ^{127}I resonances of alkali metal halides in aqueous solutions. From the concentration dependence of the chemical shifts, they concluded that the potassium, rubidium and cesium halides undergo contact ion pair formation while lithium and sodium halide ion pairs are solvent mediated at low concentrations.

COMPLEXATION STUDIES OF CRYPTANDS

As early as 1968, it has been shown that in the transport of ions through membranes (49), macrocycle compounds increase ionic permeability and selectivity for the potassium ion over the sodium ion. Since then, macrocyclic and macrobicyclic polyethers have been synthesized (50) to serve as models in the simulation of ion transport in biological systems. Cryptands are a class of bicyclic ligands first synthesized by Lehn and co-workers (51,52). The remarkable complexing ability of these diaza-polyoxamacrocycles with alkali metal ions aroused much interest in biological and chemical areas of research. Cryptands 211, 221 and 222 are shown in Figure 1. The syntheses of these cryptands are described by Lehn and co-workers (53) and Ceraso and Dye (54). The complexed form, called the cryptate, has several conformations in solution, as presented in Figure 2 for the 222 cryptate, while crystal structure studies (55-58) indicate that the complexed ligand is in the

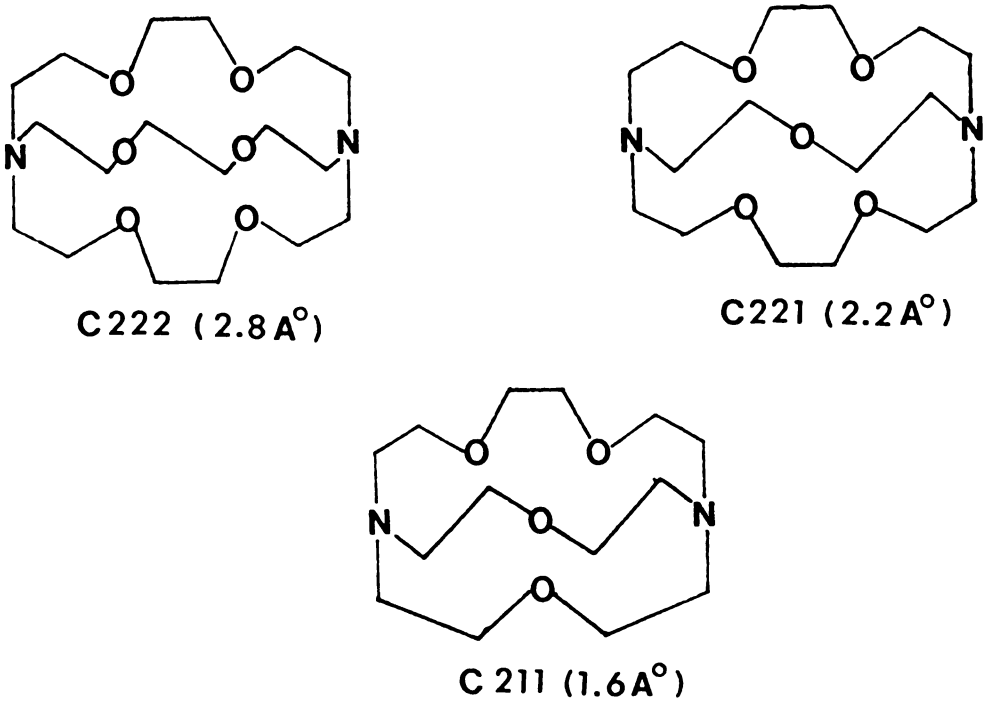

Figure 1. Cryptands C222, C221 and C211 (with internal diameters).

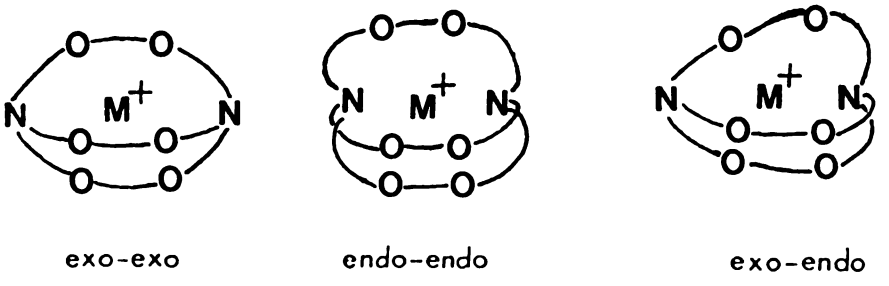

Figure 2. Conformations of the C222 Cryptand.

endo-endo form. The metal ion within the ligand cavity is stabilized by the ether oxygens and the electron pairs on the amine nitrogens.

The high selectivity and strong complexing ability of these ligands are discussed fully in a recent paper by Lehn and Sauvage (59). Cryptate stability is optimized primarily by the size relationship between the diameter of the desolvated ion and that of the three-dimensional cavity of the cryptand. Hence, the three cryptands in Figure 1 show peak selectibity for the lithium, sodium and potassium ions respectively, and the stabilities of complexes with other alkali metal ions decrease sharply. Dietrich, et al. (60) studied bivalent-monovalent cation selectivity of several cryptands for the sodium, potassium and barium ions in methanol and water solutions.

The techniques used in these complexation studies are ion-selective electrodes, potentiometry and nuclear magnetic resonance. The last method seems to be the most applicable to the study of these cryptates as alkali metal NMR is quite sensitive and totally free from chemical interferences. Lithium-7 NMR was used by Cahen (61) to study lithium cryptates C211, C221 and C222 in various solvents and he obtained stability constants for the lithium-222 cryptate in water and pyridine. Ceraso and Dye (62) used the 222 cryptand to obtain the sodium anion, which was studied by ^{23}Na NMR and x-ray crystallography (63). Dye, et al. (64) extended this method to obtain other alkali anions and used alkali metal NMR (65) to study these complexes in non-aqueous solvents. Potassium-39 NMR is presently used by Shiih (66) to study the complexation behavior of potassium cryptates and crown complexes in various solvents. Cesium complexes of cryptands and crowns (67,68) are being investigated by Mei (69) using ^{133}Cs NMR.

The kinetics of the complexation have been the subject of much research. Lehn, et al. (70) studied the temperature dependence of the proton magnetic resonance spectra of the Na^+-C222 and K^+-C222 cryptates in D_2O and reported free energies of activation and exchange rates. Shchori, et al. (71,72) showed that for the sodium dibenzo-18-crown-6 complex in dimethylformamide at ambient probe temperature, the sodium exchanges rapidly between the solvated and complexed sites. The correlation times for the sodium cryptates were determined by Kintzinger and Lehn (73) using ^{13}C and ^{23}Na NMR measurements, together with ^{23}Na quadrupole coupling constants. Ceraso and Dye (74) reported the exchange rates and activation energy of the sodium-C222 complex in ethylenediamine. The kinetics of the lithium-C211 and lithium-C221 complexes in various solvents were studied by Cahen, et al. (75) and the energies of activation were determined. It was found that the energy of activation for the release of the lithium ion from the 211 cryptate increases with an increase in the donicity of the solvent. A recent work by Loyola, et al. (76) used spectrophotometric techniques to study the kinetics of the formation of calcium cryptates in water and methanol. Murexide was used as the color indicator. Shchori, et al. (77) used the solubility technique to obtain stability constants for a series of metal complexes of the dibenzo-18-crown-6 in water. An interesting application of the complexation interaction was reported by Villermaux and Delpuech (78) who used the sodium-221 cryptate to study single ion free energies of transfer from water to methanol for the chloride salts. Another paper (79) reports the use of cryptates in a conductance study in tetrahydrofuran to investigate the phenomena of short and long range electrostatic interactions in solution.

Ligand design and structure is an actively expanding area of research: many new ligands have been synthesized with varied topology such as tricyclic polyethers (80-82). With the aid of these synthetic macromolecules, a better understanding of interactions in solutions may be achieved.

CHAPTER II

EXPERIMENTAL

SALTS

Cesium chloride, bromide, iodide and perchlorate were obtained from Alfa (purity $\geq$ 99.9%) and were dried at 180°C for 48 hours. Cesium thiocyanate (Rocky Mountain Research, Inc.) was recrystallized from absolute ethanol and vacuum dried. Cesium tetraphenylborate was prepared by a metathetical reaction between equimolar amounts of sodium tetraphenylborate and cesium chloride in a tetrahydrofuran-water mixture. The cesium tetraphenylborate precipitate was filtered and washed with conductance water until flame photometry registered sodium content on the order of conductance water. Drying was done under vacuum at 80°C for 48 hours. Cesium picrate was synthesized by an acid-base neutralization reaction between picric acid (HPi) and cesium hydroxide.

$$CsOH + HPi = CsPi + H_2O$$

The insoluble cesium picrate was filtered, recrystallized from ethanol and vacuum dried at 70°C for 5 hours. The yellow crystals decomposed at 300°C, which compares favorably with the literature (83).

CRYPTANDS

The cryptands were purchased from EM Lab., Inc. under the trade name "Kryptofix" and were used without further purification.

SOLVENTS

Reagent grade dimethylsulfoxide (J. T. Baker Co.) was dried over freshly activated Linde Type 4A molecular sieves. Absolute methanol (Baker) was refluxed over calcium hydride and fractionally distilled.

Reagent grade formamide (Matheson, Coleman and Bell, 98%) was purified by six fractional freezings. Acetonitrile (Baker) was refluxed over granulated barium oxide and fractionally distilled under dry nitrogen atmosphere. N,N-dimethylformamide (Fisher) was dried over phosphorus pentoxide. Reagent grade propylene carbonate (Aldrich) was dried over activated molecular sieves. Reagent grade acetone (Fisher) was refluxed over calcium sulfate (Drierite) and fractionally distilled. Pyridine (Fisher) was refluxed over granulated barium oxide and fractionally distilled. Nitromethane (Aldrich Gold Label) was dried over activated molecular sieves. The automatic Karl Fischer Titrator (Aquatest) was used to check water content where possible. All solvents were stored in an inert nitrogen atmosphere.

NMR SPECTROMETER

Cesium-133 NMR measurements were made on a pulsed spectrometer equipped with a Varian DA-60 magnet operating at a field of 14.09 kG. The wide band probe was based on the prototype described by Traficante, et al. (84). An external proton lock at 60 MHz was used to maintain field stability. A detailed description of the spectrometer is given elsewhere (85). Data collection and treatment were done with a Nicolet 1083 computer (with the Nicolet 293 disk drive and disk system) using the Nicolet FT-NMR (NIC-80/S-7202-D) software package. Wilmad 513-3PP 10 mm OD precision sample tubes were used.

Temperature control was achieved with continuous nitrogen flow using a Varian temperature controller. Calibration of probe temperature was done with two copper-constantin thermocouples, one of which was built into the glass insert a short distance below the sample tube

and the other placed in neat solvent in the sample tube. Temperature stability was better than $\pm 1^{o}$.

CHEMICAL SHIFT MEASUREMENTS

All cesium-133 chemical shifts reported here have been corrected for bulk susceptibility of the solvent according to the equation of Live and Chan (86):

$$\delta = \delta_{obsd} + 2\pi/3\ (\chi^{ref} - \chi^{sample}) \qquad (1)$$

for the probe geometry where the magnetic flux is at right angles to the sample tube. No correction was applied for the presence of the salt as Templeman and Van Geet (87) have shown that the contribution of the salt to the total susceptibility is neglible.

The ^{133}Cs chemical shifts at infinite dilution in water has been reported by DeWitte (27) and for convenient comparison of data, all chemical shifts are referred to the infinite dilution chemical shift of the cesium ion in water. Table 1 lists the solvents used and the respective susceptibily corrections. Positive chemical shifts correspond to diamagnetic shifts (to high field), while negative shifts indicate downfield or paramagnetic shifts, relative to the reference.

DATA TREATMENT

The fourier transform software package for the Nicolet computer has data massaging facilities such as exponential multiplication to enhance the signal-to-noise ratio. This results in some artificial line broadening but as the chemical shift is essentially unaffected, this function was routinely employed. However, for the temperature study of the three cryptates of cesium (see Chapter V), the line widths

Table 1. Corrections Applied to Cesium-133 Chemical Shift

Solvent	Volumetric Susceptibility ($\times 10^6$)	δ^{corr} ppm (relative to $\delta_o H_2O$)
Nitromethane ($MeNO_2$)	-0.391	-10.28
Acetonitrile (ACN)	-0.529	- 9.99
Propylene Carbonate (PC)	-0.640	- 9.76
Acetone	-0.460	-10.13
Formamide ($ForNH_2$)	-0.551	- 9.94
Methanol (MeOH)	-0.530	- 9.99
N,N-dimethylformamide (DMF)	-0.500	-10.05
Dimethylsulfoxide (DMSO)	-0.630	- 9.78
Water	-0.720	- 9.59
Pyridine (Py)	-0.610	- 9.82

are of great importance: consequently, the same exponential constant was used for all free induction decay signals collected unless indicated otherwise.

Data fitting was done on the CDC 6500 computer system with extensive use of KINFIT, a non-linear curve fitting program developed by Dye and Nicely (88).

CHAPTER III

A CESIUM-133 NUCLEAR MAGNETIC RESONANCE STUDY OF SOLUTIONS OF CESIUM SALTS IN VARIOUS SOLVENTS

INTRODUCTION

The nuclear magnetic resonance properties of the cesium-133 nucleus are given in Table 2. The shielding constant for a nucleus is a sum of several terms (89),

$$\sigma = \sigma_d + \sigma_p + \sigma_o \qquad (2)$$

where σ_d is the diamagnetic shielding factor arising from the induced motion of a spherically symmetric electron cloud at a nucleus approximated by Lamb's formula (90).

$$\sigma_d = \frac{4\pi e^2}{3mc^2} \int_o^\infty r\rho(r)\, dr \qquad (3)$$

However, non-spherical symmetry would result in distortion of the motion, the net effect of which is represented by the paramagnetic term, σ_p,

$$\sigma_p = \frac{-e^2\hbar^2}{m^2c^2\Delta E} \left\langle \Psi_o \left| \sum_{\nu\nu'} \frac{r^{-3}\, 2}{\partial\phi_\nu \partial\phi_{\nu'}} \right| \Psi_o \right\rangle \qquad (4)$$

where ΔE is the average excitation energy and $\frac{\partial^2}{\partial\phi_\nu \partial\phi_{\nu'}}$ is the angular momentum of the ν^{th} electron. In the case of the cesium nucleus, ΔE is small relative to the other alkali metals (91), and this fact, together with the small quadrupole moment, permit ready mixing of the ground state with excited states in the presence of an external field. As a result, the paramagnetic term contributes predominantly to the total shielding at the nucleus. The last term, σ_o, incorporates all other inter- and intra-ionic effects such as bulk magnetic susceptibility of the solvent, magnetic anisotropy of the environment and fluctuating electric field gradients due to polar effects of the surrounding

Table 2. NMR Properties of the Cesium-133 Nucleus

Natural abundance	:	100%
Spin	:	7/2 (units of h/2)
Electric quadrupole moment	:	-0.004 (units of e x 10^{-24} cm^2)
Magnetogyric ratio	:	2.5642 (units of eh/4π Mc)
Relative sensitivity	:	2.75 (constant field, compared to equal number of ^1H)
Resonance frequency	:	7.8709 MHz (in 14.09 KG field)
Natural line width	:	< 1 Hz

medium (92). The relative magnitudes and signs of these effects are difficult to determine: however, since these effects are small relative to the paramagnetic shielding at the cesium nucleus, deviation from spherical symmetry of the closed shell ion results in smaller (downfield) chemical shifts as the electron density increases. The negative sign of the σ_p term yields a more negative overall shielding constant with increasing electron density and results in a shift to lower field at constant frequency.

$$H = (1 - \sigma_{total}) H_o \tag{5}$$

$$H = \frac{(H_{ref} - H_{sample}) 10^6}{H_{ref}} \tag{6}$$

Cesium-133 nucleus has a wide range of chemical shifts and is therefore, sensitive to variations in the immediate environment. There is a unique advantage of cesium-133 NMR over conductance and other conventional techniques in monitoring solutions: because of the nature of the nuclear magnetic resonance signal, localized interactions at the resonating nucleus can be monitored to the exclusion of interactions in the bulk of the solution. The major drawback is that the lower limit of concentration that can be practically and routinely used is 0.001 M.

RESULTS AND DISCUSSION

The chemical shifts of a number of cesium salts in different solvents with respect to that of the infinitely dilute solution of cesium ions in water are given in Table 7 in Appendix I. The choice of salt and solvent were made in reference to a previous similar study

Table 3. Donor Numbers and Dielectric Constants of Solvents Used

Solvent	Donor Number	Dielectric Constant	Dipole Moment
$MeNO_2$	2.7	35.9	3.56
ACN	14.1	38.8	3.44
PC	15.1	69.0	--
Acetone	17.0	20.7	2.69
$ForNH_2$	24.7	109.5	3.37
MeOH	25.7	32.7	2.87
DMF	26.6	36.7	3.86
DMSO	29.8	45.0	3.90
H_2O	33.0	78.6	1.85
Pyridine	33.1	12.0	2.37

Table 4. Cesium-133 Chemical Shifts at Infinite Dilution in Different Solvents

Solvent	δ_o	Averaged δ_o (from ref. 27)
$MeNO_2(ClO_4^-)$	59.2 ± 0.1	59.8 ± 0.2
$ACN(I^-)$	-33.3 ± 0.6	-32.0 ± 0.4
$ACN(B\phi_4^-)$*	-34.0	
$PC(B\phi_4^-)$*	35.1 ± 0.3	35.2 ± 0.2
$Acetone(B\phi_4^-)$	26.3 ± 0.3	26.8 ± 0.3
$ForNH_2(Pi^-)$	2.30 ± 0.6	2.2 ± 0.2
$DMF(B\phi_4^-)$	0.40 ± 0.03	0.5 ± 0.2
$DMF(Pi^-)$	1.8 ± 0.1	
$DMSO(B\phi_4^-)$	-68.0 ± 0.3	-68.0 ± 0.2
$DMSO(Pi^-)$	-66.5 ± 0.5	
$H_2O(SCN^-)$	0.11 ± 0.08	0.0 ± 0.1
$Pyridine(B\phi_4^-)$	<-13	---

*E. Mei

(27) so as to further extend the characterization of cesium salts in solution. Consequently, the data obtained from this study will be discussed in conjunction with those reported by DeWitte (27) and Mei (97). Table 3 lists the donor number, dielectric constant and dipole moment of the ten solvents investigated. Figures 3 to 7 show the concentration dependence of the ^{133}Cs chemical shift in several solvents. Asterisks mark the eleven solutions from this study. The error in the measurement of the cesium chemical shift was less than ± 0.16 ppm and no appreciable broadening of the signal was observed over the concentration range studied. Extrapolation to infinite dilution was done by fitting a seventh order polynomial equation using KINFIT, a program developed by Dye and Nicely (88). The procedural details have been discussed elsewhere (93). The chemical shifts at infinite dilution are compared with those obtained by DeWitte in Table 4 and they seem to agree well.

Of the alkali metal ions, the cesium ion is the most poorly solvated because of the lower charge density of the large cesium cation. Long range interactions are expected to be negligibly weak as a result of the small charge-to-size ratio. Hence, the concentration dependence of the cesium-133 chemical shift should reflect ionic interactions within the primary solvation sphere. From Figures 3 to 7, it can be seen that, in any one solvent, increasing concentration of salt can lead to upfield or downfield chemical shifts. Tetraphenylborate and perchlorate salts belong to the former and the other five anions, picrate, thiocyanate, chloride, bromide and iodide are in the latter group. (There is one exception - cesium perchlorate in nitromethane shifts <u>downfield</u> with increasing concentration. This case will be

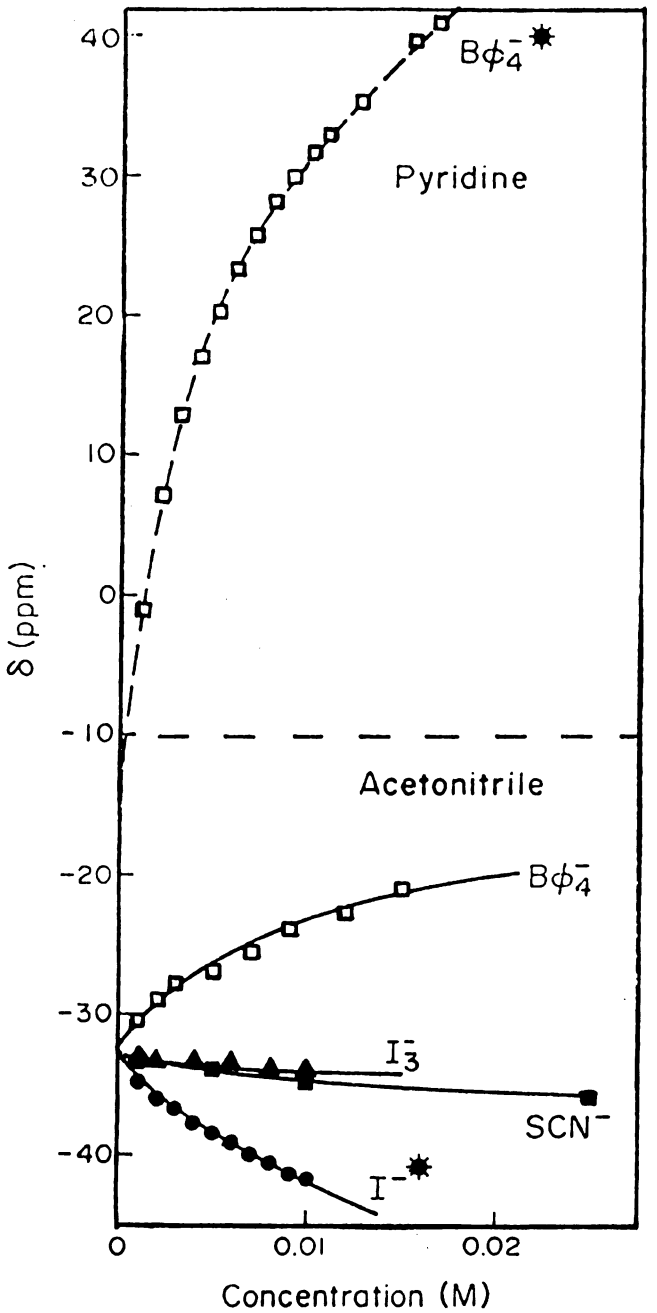

Figure 3. Concentration Dependence of the ^{133}Cs Chemical Shifts of Cesium Salts in Pyridine and Acetonitrile. ✸ indicates data from this study.

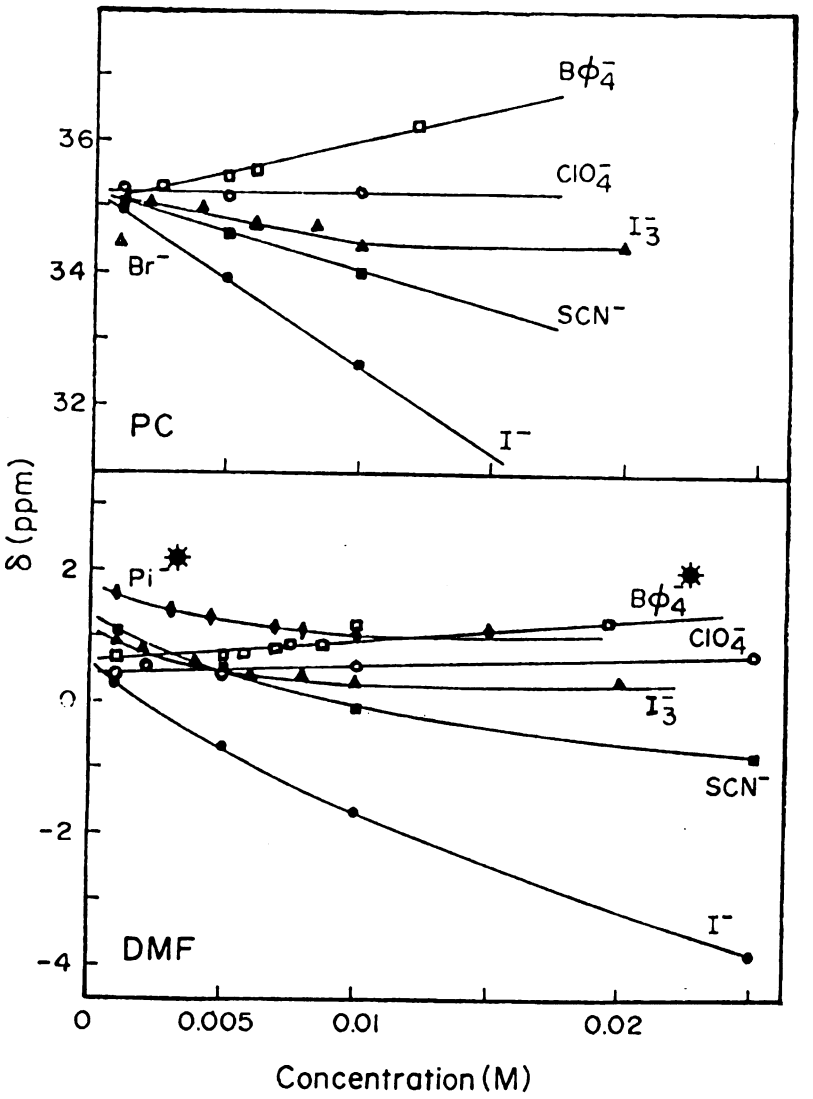

Figure 4. Concentration Dependence of the ^{133}Cs Chemical Shifts of Cesium Salts in PC and DMF. ✸ indicates data from this study.

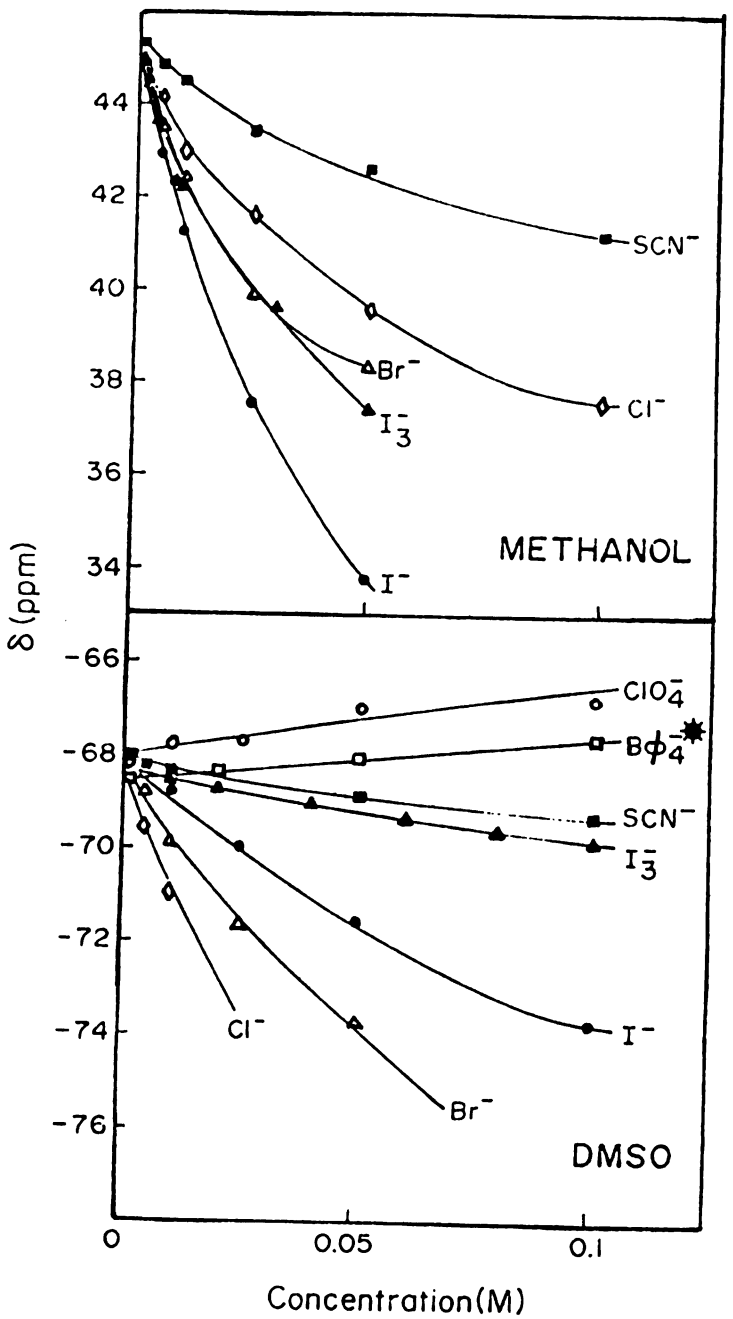

Figure 5. Concentration Dependence of the ^{133}Cs Chemical Shifts of Cesium Salts in Methanol and DMSO. ✸indicates data from this study.

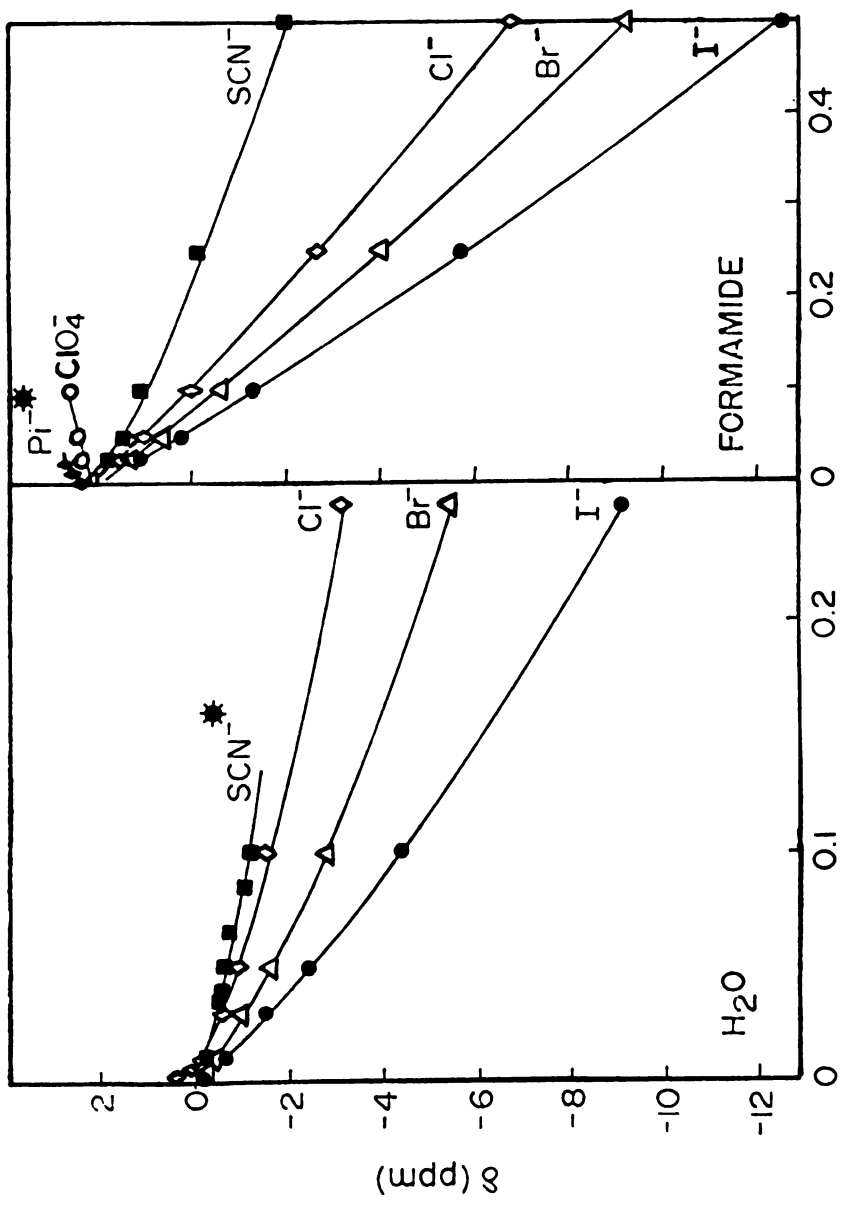

Figure 6. Concentration Dependence of the ^{133}Cs Chemical Shifts of Cesium Salts in H_2O and Formamide. ✱indicates data from this study.

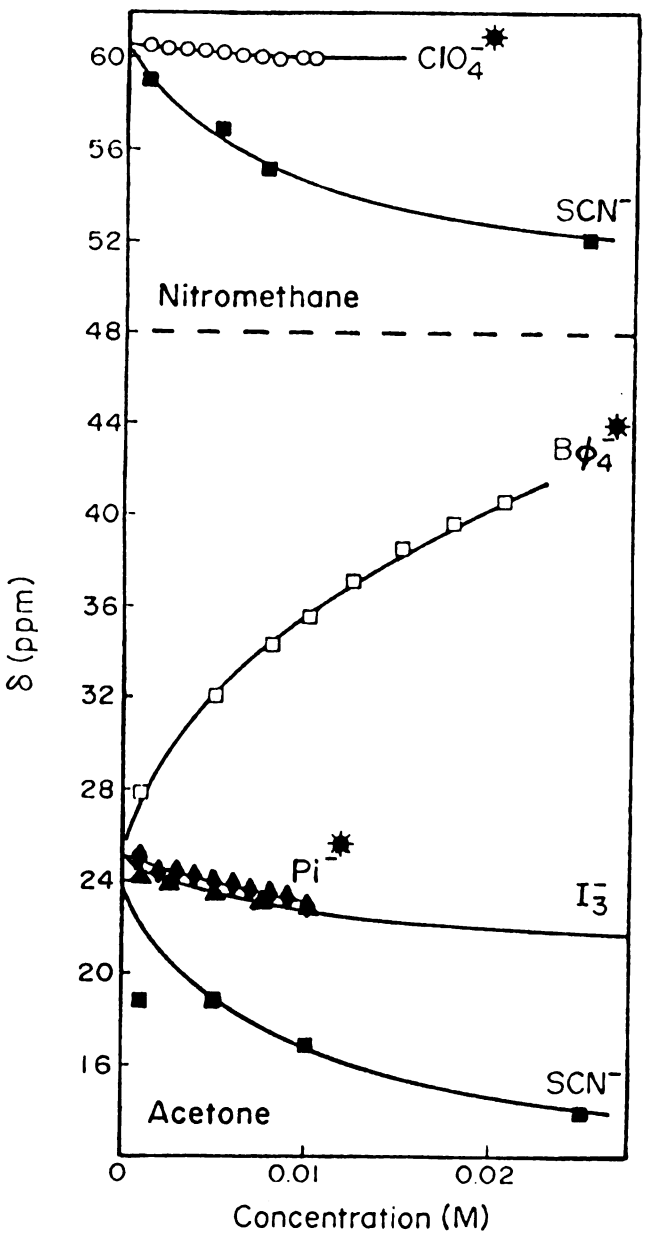

Figure 7. Concentration Dependence of the ^{133}Cs Chemical Shifts of Cesium Salts in $MeNO_2$ and Acetone. ✸ indicates data from this study.

duly discussed.) From the change in chemical shift, it can be seen that the size, symmetry and type of anion play an important role in ion association as a result of the small interaction energy of solvation. At infinitely dilute concentrations, the cesium ion is completely solvated by the solvent molecules, and the chemical shift characteristic of the electron donating ability of the solvent is observed. However, upon increasing the salt concentration, the solvent-cation interaction is gradually replaced by cation-anion interaction and the formation of solvent separated and/or contact ion pairs. In the latter case, the electron density at the nucleus is either decreased or increased relative to the free solvated state. For the bulky, symmetric tetraphenylborate and perchlorate anions, it appears that the electron density is indeed decreased, leading to an upfield shift, whereas the thiocyanate, picrate, triiodide and halide anions act as better electron donors than the solvent molecule(s) displaced. From equation 4 (page 15), it can be seen that the paramagnetic shielding term is a function of the angular momentum of the electrons. Solvent-cation interaction would reduce the symmetry of the closed shell configuration of the cesium ion and induce some angular momentum as the outer orbitals of the cesium ion are overlapped with the appropriate molecular orbitals of the solvent. With the approach of the anions giving downfield shifts, this effect is even more pronounced due to the polarizability (in the case of the halides) and localized negative charge (in the case of the picrate and thiocyanate ions) of the anions, resulting in paramagnetic shifts.

The exception noted above in the case of cesium perchlorate in nitromethane indicates that in this solvent of low donicity, the

perchlorate anion, even with its reduced charge density, is a better donor of electrons than is the solvent molecule displaced and the net effect observed on the NMR time scale is a shift to low field.

Solvent effect on the cesium-133 chemical shift is graphically presented in Figure 8 for the tetraphenylborate salt and in Figure 9 for the thiocyanate salt. (Cesium thiocyanate is soluble in more solvents than the other cesium salts used in this study.) There is a noticeable trend in the range of chemical shifts of cesium thiocyanate in each solvent. In oxygen donor solvents, nitromethane, methanol, propylene carbonate and acetone, the ^{133}Cs chemical shifts are upfield relative to nitrogen solvents, dimethylformamide, formamide, acetonitrile and pyridine. Dimethylsulfoxide, being a solvent of high donicity and relatively high dielectric constant, apparently solvates the cesium ion very efficiently, giving the most downfield shifts and futhermore, little concentration dependence is observed. A similar trend is found for the tetraphenylborate salt, except in the two solvents acetone and pyridine. In these two solvents, increasing salt concentration produces considerable change in electron density at the cesium ion. These results seem to imply that the presence of the anion is very much more significant for this salt over the concentration range studied than is found to be the case in the other solvents.

A glance at Table 3 will help explain the trends observed above. Acetone and pyridine have the lowest dielectric constants and dipole moments of all the solvents used. Consequently, the large, symmetrical tetraphenylborate ion can readily approach the cesium ion even at low concentrations as a result of the low dielectric of the medium, giving rise to appreciable curvature in the plots.

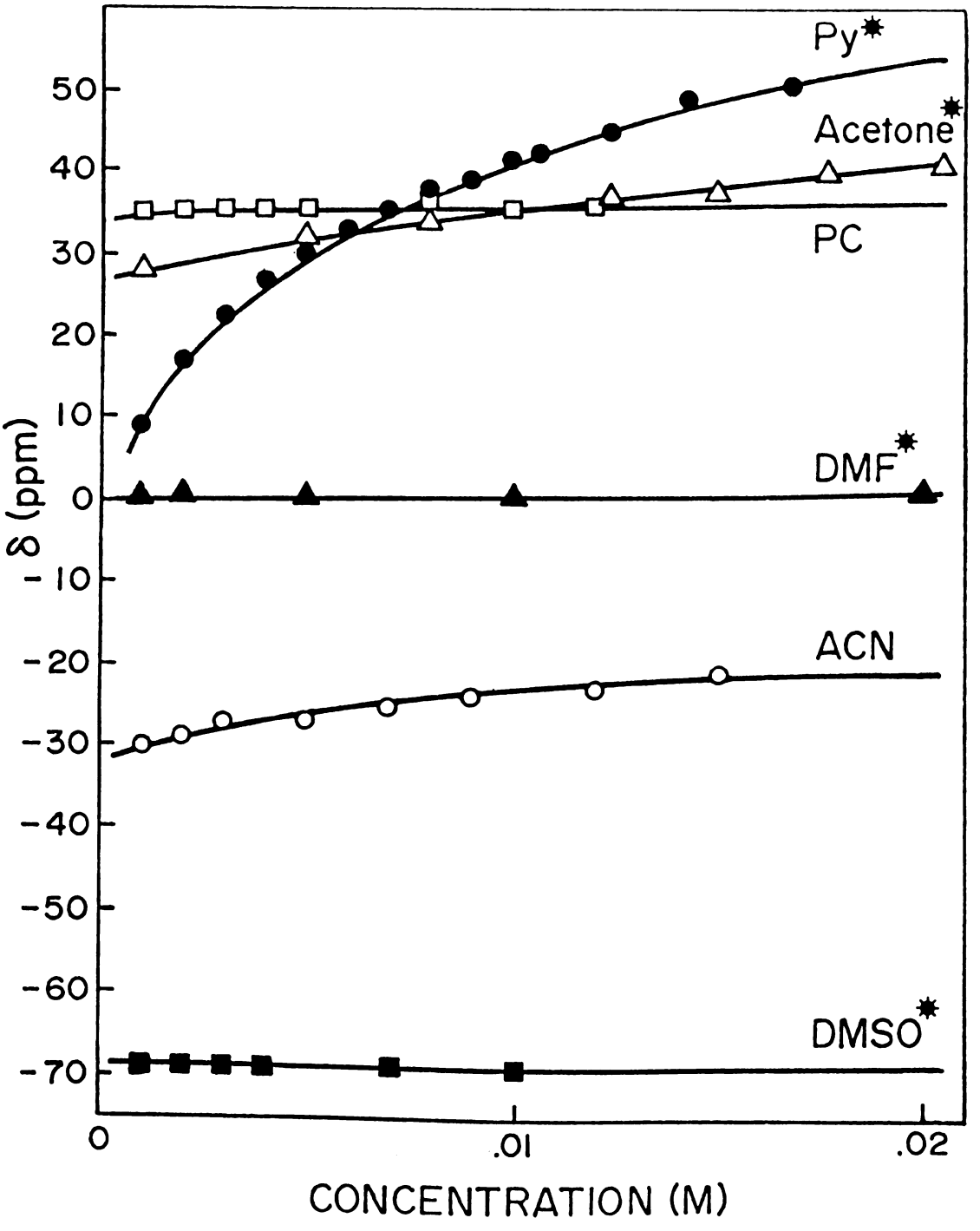

Figure 8. Concentration Dependence of the ^{133}Cs Chemical Shifts of $CsB\phi_4$ in Various Solvents. * indicates data from this study.

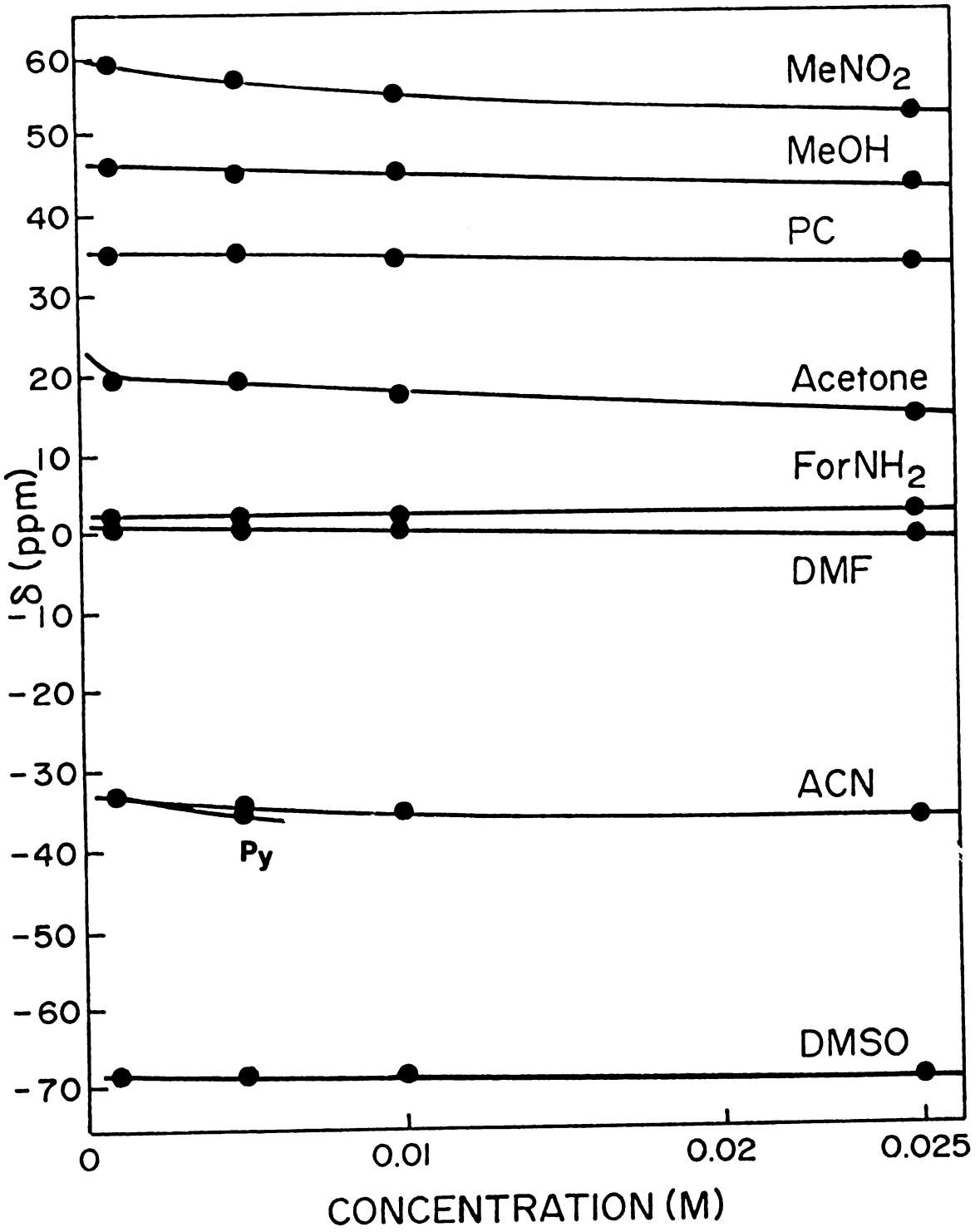

Figure 9. Concentration Dependence of the ^{133}Cs Chemical Shifts of CsSCN in Various Solvents.

In cases where the solubility of the salt is equal to or greater than 0.01 M, the ion pair formation constant was determined using the program KINFIT. This method has been described elsewhere (93). The values obtained are reported in Table 5 together with those from the work done by DeWitte (93).

The association constants for CsSCN in different solvents are listed in Table 5 in the order of increasing donor ability of the solvent. It appears that as the donicity of the solvent decreases, ion pair association increases with one exception - water. A possible rationale is that water is a highly structured solvent with extensive hydrogen bonding and the introduction of a solute into the bulk medium apparently results in structure breaking effects leading to a greater degree of association than is otherwise expected.

$CsB\phi_4$ in DMF and DMSO is negligibly associated. These two solvents are good donor solvents and thus inhibit ionic association. The ion pair formation for this salt in ACN and PC are larger than the corresponding values for the CsSCN ion pair, which is rather surprising. One can only speculate that the cesium ion could have remarkable affinity to the tetraphenylborate anion as a result of unique structural orientation to the phenyl rings on the anion. Another point of interest is the high degree of ionic association of the tetraphenylborate salt in pyridine. Due to pronounced curvature of the plot (see Figure 3), it is difficult to extrapolate to infinite dilution in pyridine. However, it was established that the ion pair formation constant is greater than 100. One can infer that the aromaticity of the strong donor solvent, pyridine, stablilizes the ion pair. The association constant for the tetraphenylborate salt in PC is 12.0 $\pm$ 7.2

Table 5. Ion Pair Formation Constants of Cesium Salts in Various Solvents

Anion	Solvent	K_{ip}	
SCN^-	Nitromethane	44.1 ± 1.2	
	Acetonitrile	13.2 ± 3.8	
	Propylene Carbonate	3.4 ± 0.5	
	Methanol	3.9 ± 0.6	
	Dimethylformamide	1.1 ± 0.2	
	Dimethylsulfoxide	1.6 ± 0.5	
	* Water	3.3 ± 1.6	
$B\phi_4^-$	Acetonitrile	53.5 ± 13.7	**
	Propylene Carbonate	12.0 ± 7.2	**
	* Acetone	25.4 ± 1.9	**
	* Dimethylformamide	∿ 0	**
	* Dimethylsulfoxide	∿ 0	**
	* Pyridine	$>10^2$	**
Cl^-	Methanol	9.1 ± 1.9	
Br^-	Methanol	40.0 ± 7.1	
I^-	Acetonitrile	34.0 ± 4.9	
	Methanol	15.3 ± 0.9	

* From this work.

** Averaged values from two sets of experiments.

which is unexpectedly smaller than that in acetone. If the donor ability of solvent is the dominant factor present, one would expect ionic association to be stronger in a lower donor solvent such as PC. However, PC has a high dielectric constant and this fact probably accounts for the smaller ion pair formation constant.

The halides appear to be associated in varying degrees in methanol. Instead of the expected trend of increasing ion pair formation with increasing "softness" of the anion, the results follow the trend $Cl^- < Br^- > I^-$. The iodide ion is isoelectronic with the cesium ion and, therefore, ion pair formation should be strongest compared to the three halides. However, the results indicate otherwise.

CHAPTER IV

CESIUM-133 NMR STUDY OF CESIUM COMPLEXES WITH CRYPTANDS C211, C221 AND C222 IN NON-AQUEOUS SOLVENTS

INTRODUCTION

Since the advent of bicyclic diaza-polyoxamacrocyclic compounds (cryptands) synthesized by Lehn and co-workers in 1969 (53), much interest has been shown in the complexing behavior of these ligands with alkali metal ions in various solvents. Cesium-133 NMR is used in this study to monitor the complexation interaction of the cesium ion with the cryptands C211, C221 and C222 in various non-aqueous solvents.

CESIUM-C211 CRYPTATES

^{133}Cs chemical shifts were determined as a function of cryptand to cesium ion mole ratio (MR). The results are shown in Figures 10 to 14 and Table 8 in Appendix I. Cesium ion concentration is maintained at 0.01 M. The estimated error in the measurements is ± 0.01 ppm. The line widths observed show a slight increase from about 5 Hz to 10 Hz (subject to the inhomogeneity of the field) with increasing ligand concentration. Cesium tetraphenylborate-C211 complex in acetone was studied up to a mole ratio of 20. The reaction appears to be less than quantitative even with a large excess of ligand, which is not unexpected considering the small ligand cavity (0.8 A radius, endo-endo form) (94), and the size of the cesium ion (1.84 A radius). The C211 ligand show peak selectivity for the lithium ion, with which it forms a strong, inclusion complex, i.e. the metal ion is centrosymmetric within the ligand cavity. This cryptand has been studied by Cahen, et al. (75), who showed that the lithium-7 chemical shift of the complex is essentially independent of solvent and counterion.

Cation exchange between the two sites (free and complexed) is slow on the NMR time scale since two resonances of ^{7}Li nucleus were observed when the metal ion was present in excess.

From Figures 11 to 14, it can be seen that the downfield chemical shifts are very much dependent on solvent and anion and that, in most cases, the plots show very little curvature as a consequence of the extremely weak cation-ligand interaction. In DMSO, a solvent of high donicity and relatively high dielectric constant, no evidence of complexation was observed for the cesium tetraphenylborate salt and cryptand C211. Apparently, the strongly interacting primary solvation sphere excludes the C211 cryptand effectively even at a 5:1 excess of the ligand. On the other hand, complexation interaction is greatest for the thiocyanate salt in nitromethane, a solvent of low donicity. The poor donor ability of the solvent molecules, together with the low charge-to-size ratio of the cesium ion enable the electrically neutral ligand to approach and coordinate to the cesium ion. The chemical shift varies over a wide range (almost 40 ppm) and a greater degree of curvature is observed.

Figure 14 shows the complexation of cesium chloride, perchlorate and picrate salts with C211 in various solvents. The picrate salt was sufficiently soluble in only three solvents, formamide, dimethylformamide and dimethylsulfoxide, all of which are good donor solvents. Consequently, little complexation was observed as indicated by the almost linear, horizontal mole ratio plot for the complex in DMF solution shown in Figure 14. Slight curvature is observed for the MR plot of cesium chloride-C211 complex in methanol while the cesium perchlorate-C211 cryptate in nitromethane exhibited pronounced

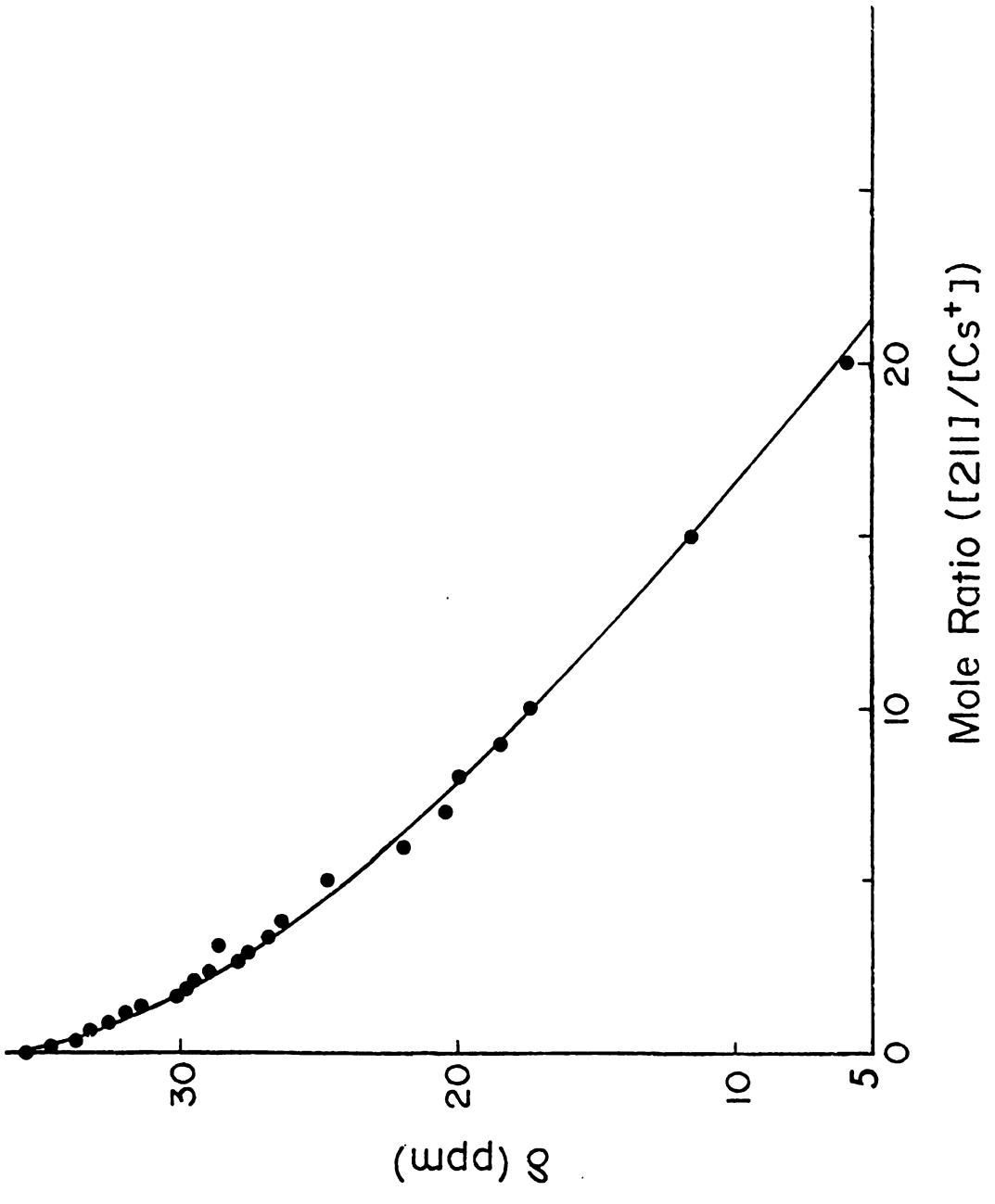

Figure 10. ^{133}Cs Chemical Shifts of $CsB\phi_4$-C211 Cryptate in Acetone.

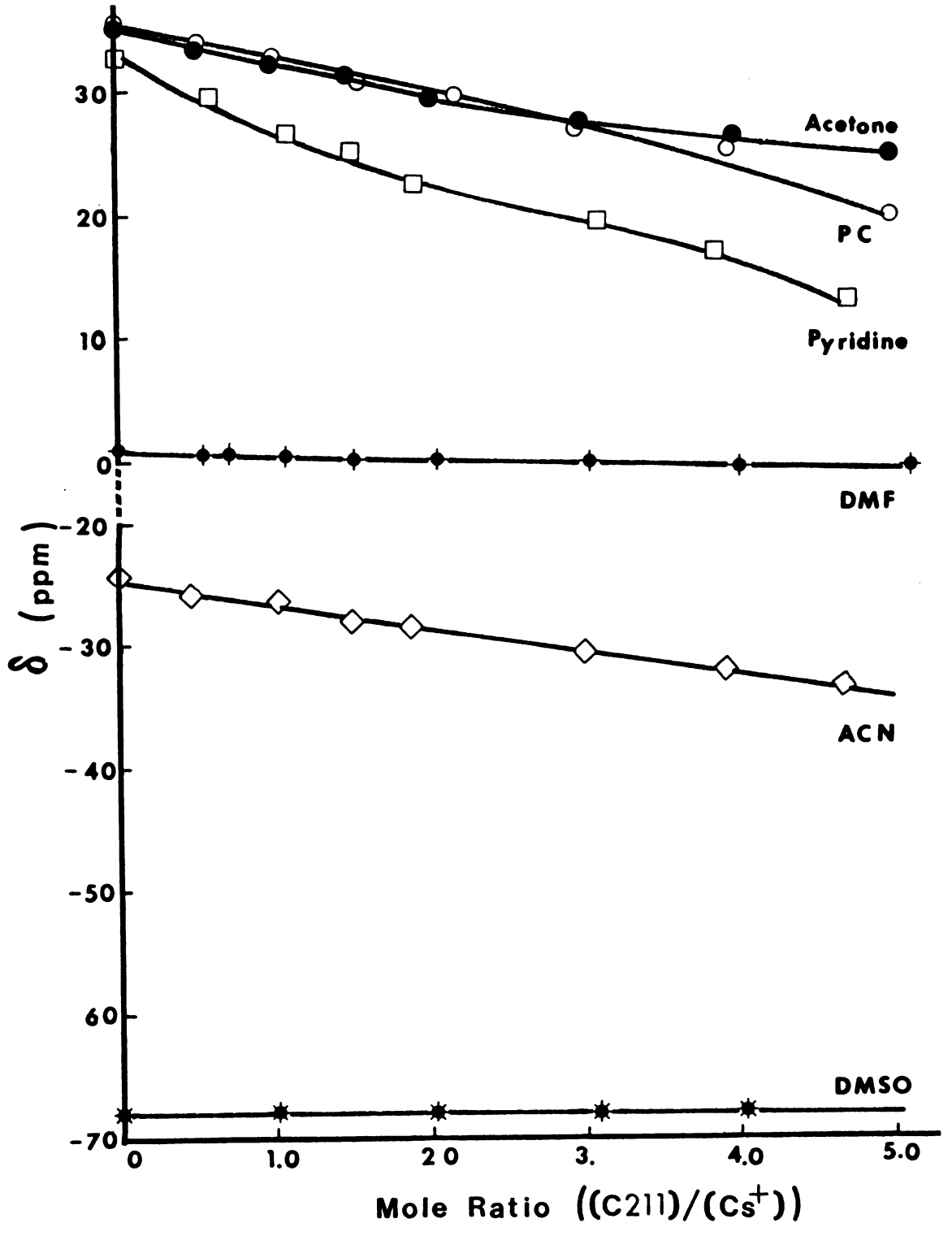

Figure 11. ^{133}Cs Chemical Shifts of $CsB\phi_4$-C211 Cryptate in Various Solvents.

Figure 12. ^{133}Cs Chemical Shifts of CsSCN-C211 Cryptate in Various Solvents.

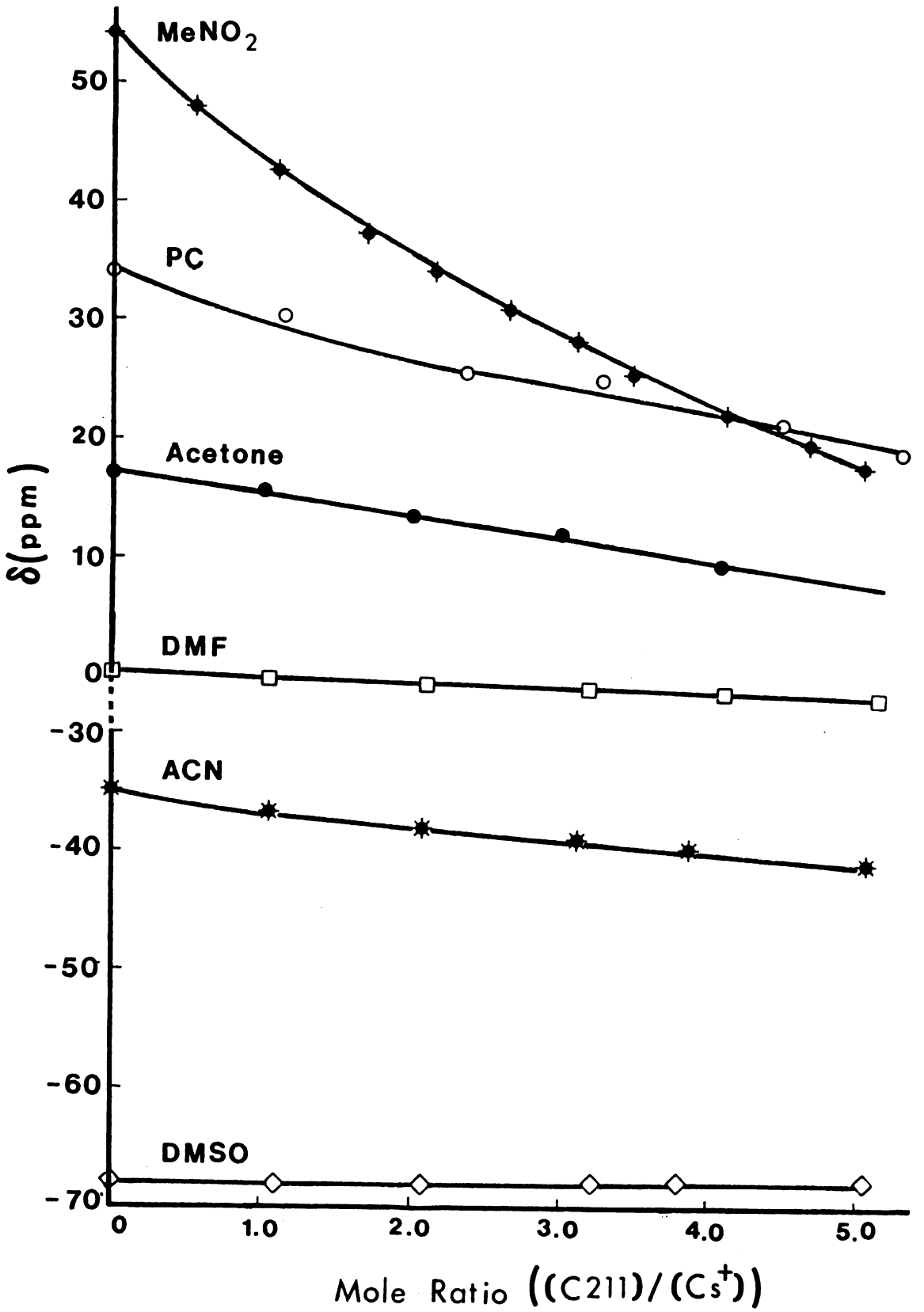
MeNO2
PC
Acetone
DMF
ACN
DMSO
δ(ppm)
50
40
30
20
10
0
-30
-40
-50
-60
-70
0
1.0
2.0
3.0
4.0
5.0
Mole Ratio ((C211)/(Cs+))

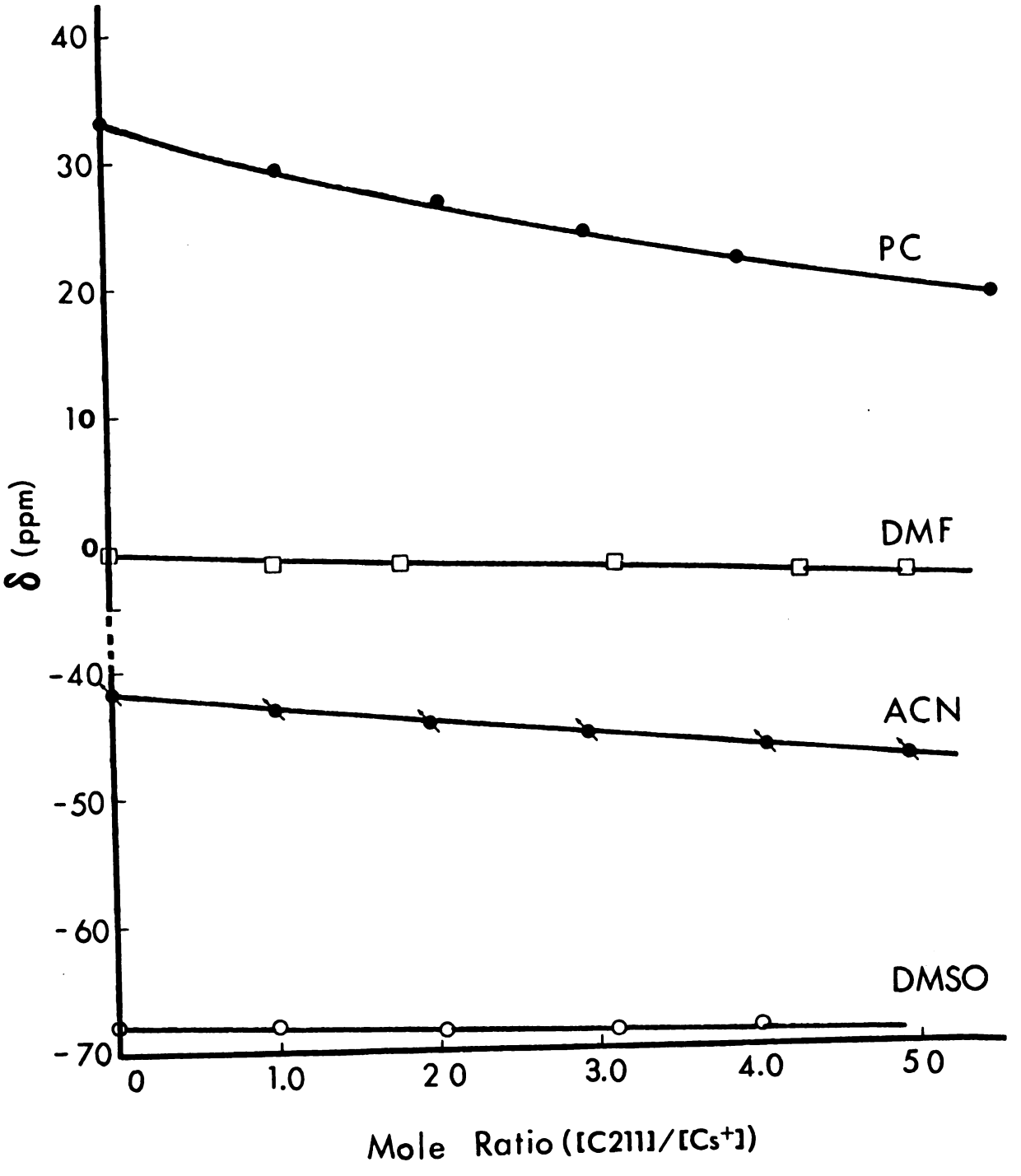

Figure 13. ^{133}Cs Chemical Shifts of CsI-C211 Cryptates in Various Solvents.

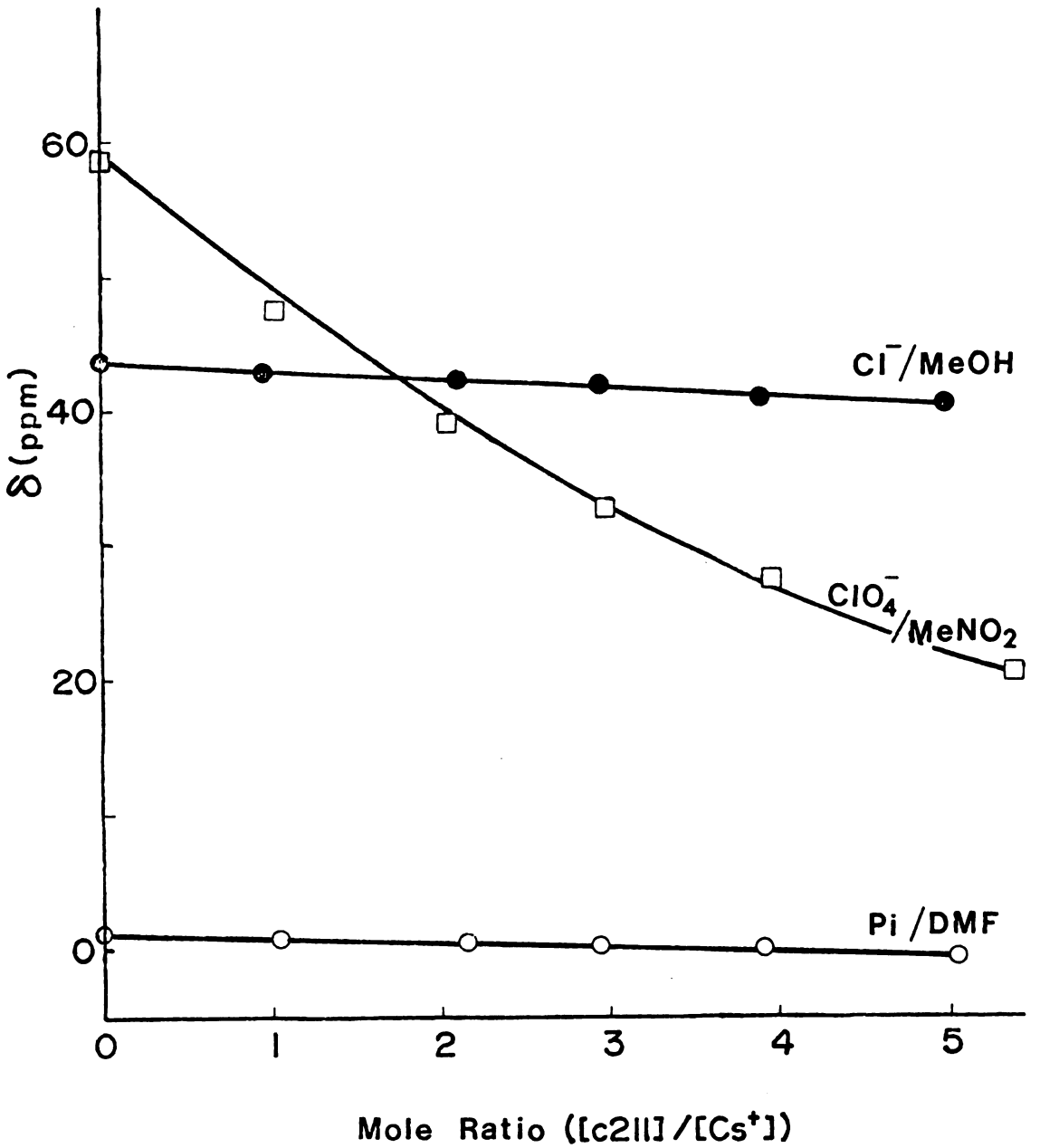

Figure 14. ^{133}Cs Chemical Shifts of Cesium-C211 Cryptates in Various Solvents.

curvature. The complex in nitromethane is significantly stronger than in other solvents as the cesium perchlorate ion pair is negligibly associated (see Chapter III) in this poor donor solvent and complexation is stabilized.

In solutions where complexation does occur, the following equilibria are in effect:

$$M^+ + A^- = M^+A^-$$

$$M^+ + L = (ML)^+$$

The cesium ion and cryptand C211 must form an exclusion complex since the relative sizes of the metal ion and ligand cavity would prohibit the entry of the ion into the central cavity. It is interesting to note that the chemical shift values at high concentrations of ligand do not appear to converge to a chemical shift value characteristic of the cesium ion within the ligand cavity as they do for ^7Li chemical shifts in the Li^+-C211 complex (97). The mole ratio plots exhibit smooth curvature and no abrupt change in chemical shift was noted which would indicate a change in stoichiometry of the complex as a result of coordination to a second ligand.

Assuming that only cation-ligand interactions are important, the observed ^{133}Cs chemical shift is a population average of the two chemical environments of the cesium ion.

$$\delta_{obsd} = x_M\delta_M + x_{ML}\delta_{ML} \qquad (7)$$

where δ_M and δ_{ML} are the chemical shifts characteristic of the solvated and complexed metal ions respectively, and x_M and x_{ML} are the corresponding mole fractions. Using this model, an expression can be derived for the observed chemical shift to which the experimental data are fitted to obtain a value for the concentration formation constant

(61). This is accomplished with the help of the KINFIT program. The results are given in the first column in Table 6 and a sample of the computer fitting obtained for the cesium perchlorate-C211 complex in nitromethane is presented in Figure 15.

However, comparison with ion pair formation constants reported in Chapter II (also included in Table 6, column 2 for convenience) make it quite apparent that this approach is too naive as the "formation constants" of the cryptates are on the same order as the ion pair constants. In other words, the anion should be taken into consideration as both ligand and anion compete for the cesium ion in solution, and the change in the observed chemical shift is partly due to changes in the degree of anionic association with the cesium ion upon complexation. The observed chemical shift therefore, is modified to include a third factor, the chemical shift characteristic of the ion pair:

$$\delta_{obsd} = x_M\delta_M + x_{ML}\delta_{ML} + x_{MA}\delta_{MA} \quad (8)$$

The derivation of the final expression for the observed chemical shift can be obtained by applying the following equations,

$$K_{ip} = [MA]/[M][A] \quad (9)$$

$$K^f = [ML]/[M][L] \quad (10)$$

$$C_L = [ML] + [L] \quad (11)$$

$$C_M = [ML] + [M] + [MA] \quad (12)$$

$$C_M = [MA] + [A] \quad (13)$$

where K_{ip} is the ion pair association constant, K^f is the formation constant of the complex, [MA], [M] and [A] are the concentrations of the ion pair, free metal ion and free anion respectively, and C_L and

Table 6. Formation Constants of Cs^+-C211 Cryptates.

Salt	Solvent	K^f	K_{ip}	K_c^f
$CsB\phi_4$	ACN	13.9 ± 2.6	53.5 ± 13.7	43.4 ± 16.7
	PC	5.5 ± 1.8	12.0 ± 7.2	5.4 ± 2.1
	Acetone	2.8 ± 0.3	25.7 ± 1.9	4.2 ± 0.5
	DMF	16.9 ± 5.4	< 1.0	---
	Py	12.9 ± 3.5	>121.9 ± 7.5	0.5 ± 7.2
	DMSO	∿ 0	∿ 0	∿ 0
CsSCN	$MeNO_2$	18.4 ± 0.7	44.1 ± 1.2	24.4 ± 1.2
	ACN	11.1 ± 2.5	13.2 ± 3.8	21.4 ± 8.0
	PC	9.0 ± 5.4	3.9 ± 0.7	---
	Acetone	0.5 ± 0.8	---	---
	DMF	∿ 0	∿ 0	∿ 0
	DMSO	∿ 0	∿ 0	∿ 0
CsI	ACN	3.1 ± 2.3	34.0 ± 4.9	6.3 ± 3.3
	PC	6.3 ± 0.1	---	---
$CsClO_4$	$MeNO_2$	12.9 ± 0.4	∿ 0	---
CsCl	MeOH	---	9.1 ± 1.9	< 1

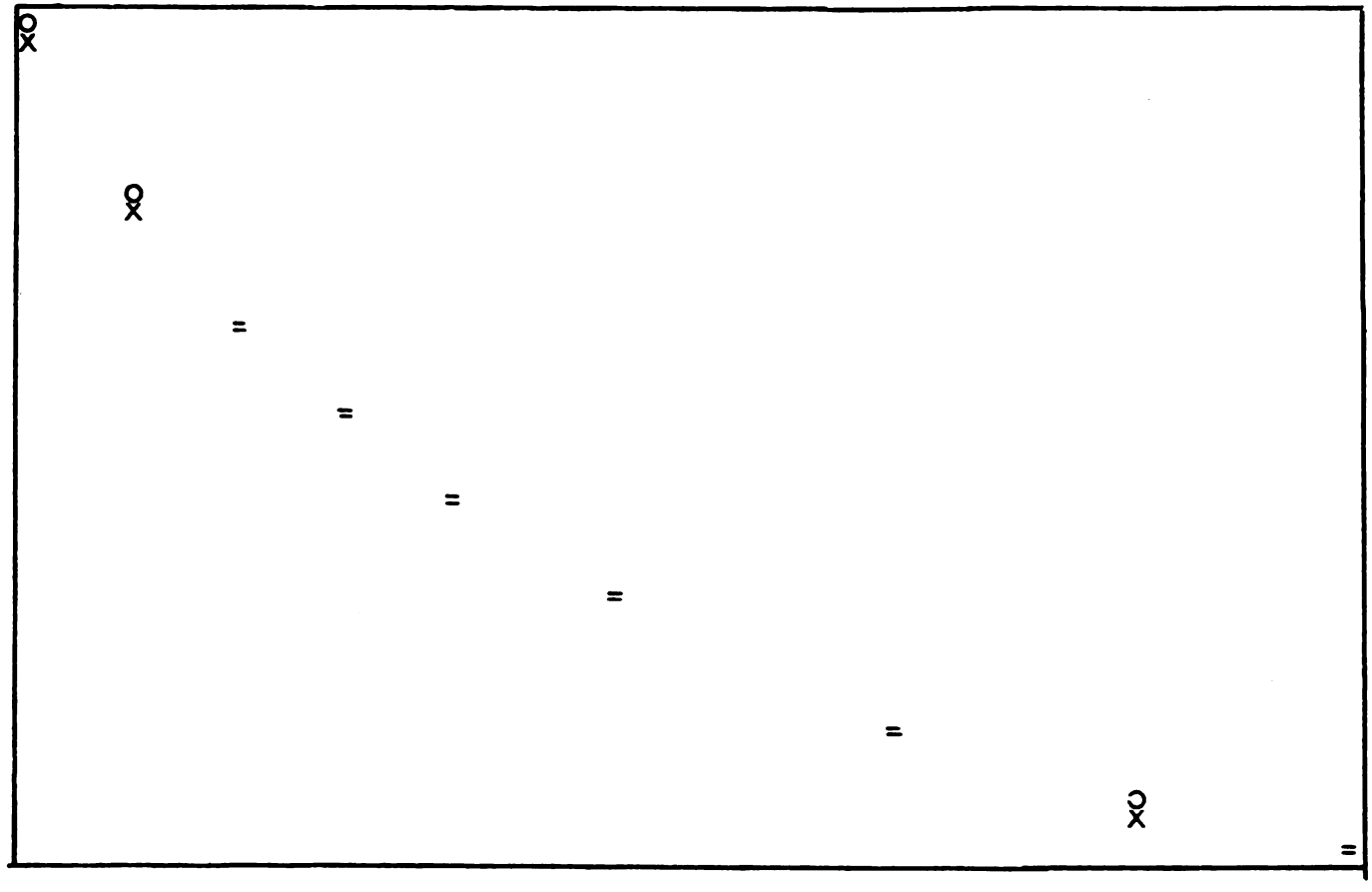

Figure 15. Computer fit of the ^{133}Cs Chemical Shifts of $CsClO_4$-C211 Cryptate in $MeNO_2$.
X means an experimental point, O means a calculated point, = means an experimental and calculated point are the same within the resolution of the plot.

C_M are the analytical concentrations of the ligand and salt. With these five equations and simple algebraic manipulations, the following expression is readily derived.

$$K^f K_{ip}[M]^3 + (K^f K_{ip} C_L + K_{ip} + K^f)[M]^2 + (K^f C_L + 1 - K^f C_M)[M] - C_M = 0 \quad (14)$$

A detailed derivation and the subroutine EQN used in KINFIT is given in Appendix II. In order to use this model, the ion pair formation constant has to be known. Using the values reported in Chapter III, eight complexes were fitted to this equation and better formation constants were obtained (Table 6, column 3).

The formation constants of the thiocyanate-C211 complex in the six solvents studied show a trend analogous to that of ion pairing, i.e. the stabilities increase with decreasing donor ability of the solvent as the weak complex is stabilized by the low donor medium. However, this is not observed for the cesium tetraphenylborate-C211 cryptates. It is interesting to note that the complexation is very weak with the cesium halides. In fact, in methanol, negligible complexation is found with cesium chloride while the cesium iodide-C211 cryptate is somewhat more stable. These results support the contention that the anion and cryptand are indeed competing for the cesium ion and in the case of the halides, the anion coordinates better to the cation than does the neutral ligand. The competitive formation constant for the cesium tetraphenylborate-C211 complex in pyridine is extremely small. Therefore, it is apparent that the curvature in the mole ratio plot is the result of changes in the ion pair equilibrium as the weak complex is formed.

CESIUM-C221 AND CESIUM-C222 CRYPTATES

From the above results, it seems quite evident that for the weak cesium-C211 complex, the anion and the solvent can have strong influence on the complexation interaction. The ligand effect is studied here with the tetraphenylborate salt. The C221 cryptand has a larger cavity size (1.1 A radius, endo-endo form) (94) than the C211 cryptand and one would expect that it would form a stronger complex with the cesium ion. The results show that the Cs^+-C221 cryptate is indeed stronger than the corresponding complex with the C211 cryptand. The data are presented in Table 9 in Appendix I and are plotted in Figure 16.

The most striking difference between these plots and those shown in Figures 11 to 14 is that in propylene carbonate, acetone, acetonitrile and pyridine, quantitative complexation is achieved around a mole ratio (defined as the concentration of ligand over the concentration of metal ion) of 1. Extrapolation of the linear portions of the plots yield an intersection at equal concentrations of metal ion and ligand (MR = 1) which indicates the formation of a 1:1 complex. The line widths in the exchange region (0<MR<1) in acetone, PC and ACN show much broadening, from less than 10 Hz to over 100 Hz. In pyridine, the exchange broadening is such that no signal was detected in the region indicated by the broken line in Figure 16. However, as the mole ratio approaches 1, most of the cesium ion is essentially complexed and the line width decreases as the limiting line width of the complexed cesium ion is reached. An attempt to obtain the formation constant of the Cs^+-C221 complex in ACN gave poor results ($K^f \approx 10^7$) as the complex is too strong.

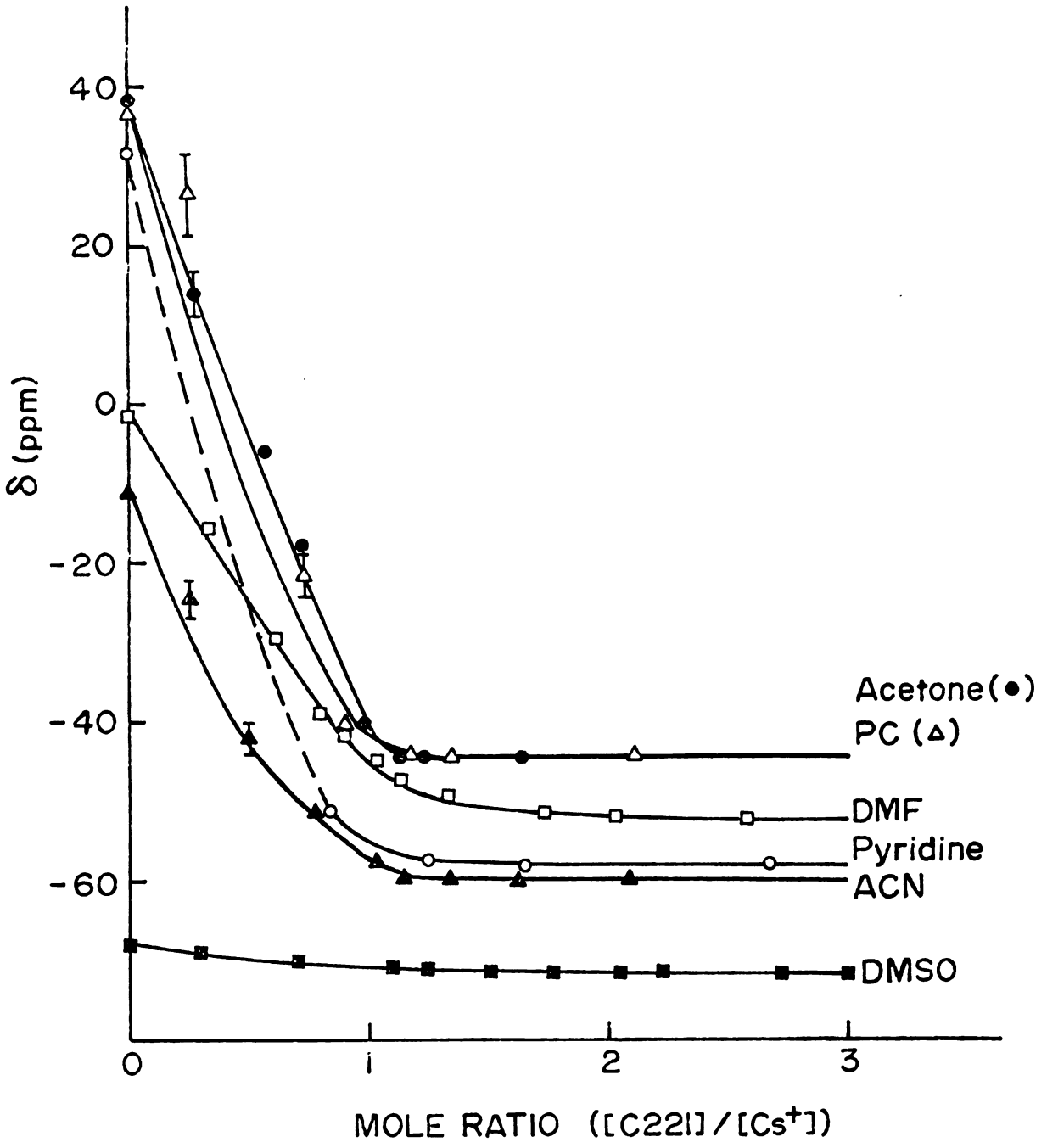

Figure 16. ^{133}Cs Chemical Shifts of $CsB\phi_4$- C221 Cryptates in Six Solvents. MR = $[C221]/[Cs^+]$.

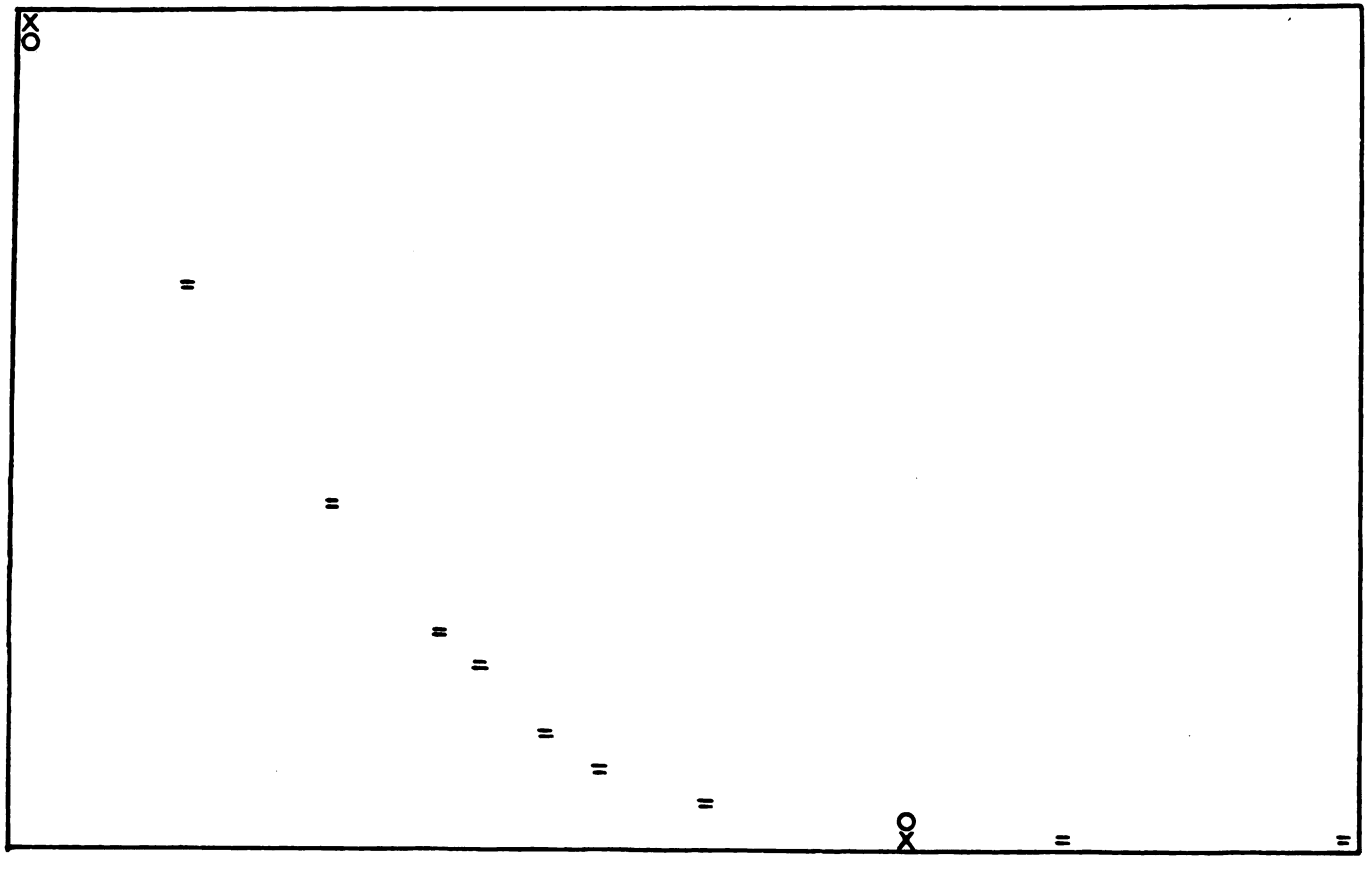

Figure 17. Computer fit of the ^{133}Cs Chemical Shifts of $CsB\phi_4$-C221 Cryptate in DMF. X means an experimental point, O means a calculated point, = means an experimental and calculated point are the same within the resolution of the plot.

In DMSO and DMF, two solvents of high donicity and medium dielectric constant, complexation is very much weaker as shown by the reduced curvature of the plots. The stability constants were readily determined with the help of the KINFIT program. The Cs^+-C221 complex in D is given in Figure 17 as an example of the computer fit obtained. The formation constants in DMF and DMSO are: $\log K_{DMF} = 3.33 \pm 0.04$ and $\log K_{DMSO} = 2.94 \pm 0.24$ respectively.

The chemical shifts characteristic of the complex are not independent of solvent and one can conceive of a complexed state whereby the cesium ion is partially occluded within the ligand cavity and partially solvated. The C221 ligand would be expected to be a good electron donor due to the multiple donor sites - 5 oxygen and 2 nitrogen atoms. The shift to low field of ^{133}Cs resonance reflects an increase in electron density at the nucleus upon complexation. Since the complex is composed of the cesium ion, ligand and solvent molecules, one would expect the chemical shift of the complex to parallel somewhat the donor ability of the solvent. This is not the case and, therefore, other factors must influence the shift, e.g. solvent structure, dielectric constant, ring currents (in the case of pyridine), etc. The range of chemical shifts between the free and complexed cesium ions give a semi-quantitative idea of the energy difference between the cesium environments. Assuming the same activated state or energy barrier of the transition, a larger range reflects a lower energy state of the complex. Greatest range of ^{133}Cs chemical shifts are observed in PC, acetone and pyridine and hence, the strongest complexes.

The ligand effect is extended to the C222 cryptand in pyridine. The results are given in Table 10 in Appendix I and in Figure 18. Again, the broken line indicates the region where the signal is broadened significantly and is beyond the detectability limit of the spectrometer. The larger C222 cryptand (1.4 A radius, endo-endo form) (94) would permit the cesium ion to enter the three dimensional cavity much more readily and the complex formed would be the most stable. The 1:1 complex has a chemical shift of -224.15 ppm (compared to -57.90 ppm for the C221 cryptate) in pyridine, indicating the high electron density at the cesium nucleus and the total range of chemical shifts is a remarkable 250 ppm. Furthermore, all the cesium ions are essentially complexed at a mole ratio of 1. The cesium-C222 cryptate in various solvents is studied in greater detail by Mei (96).

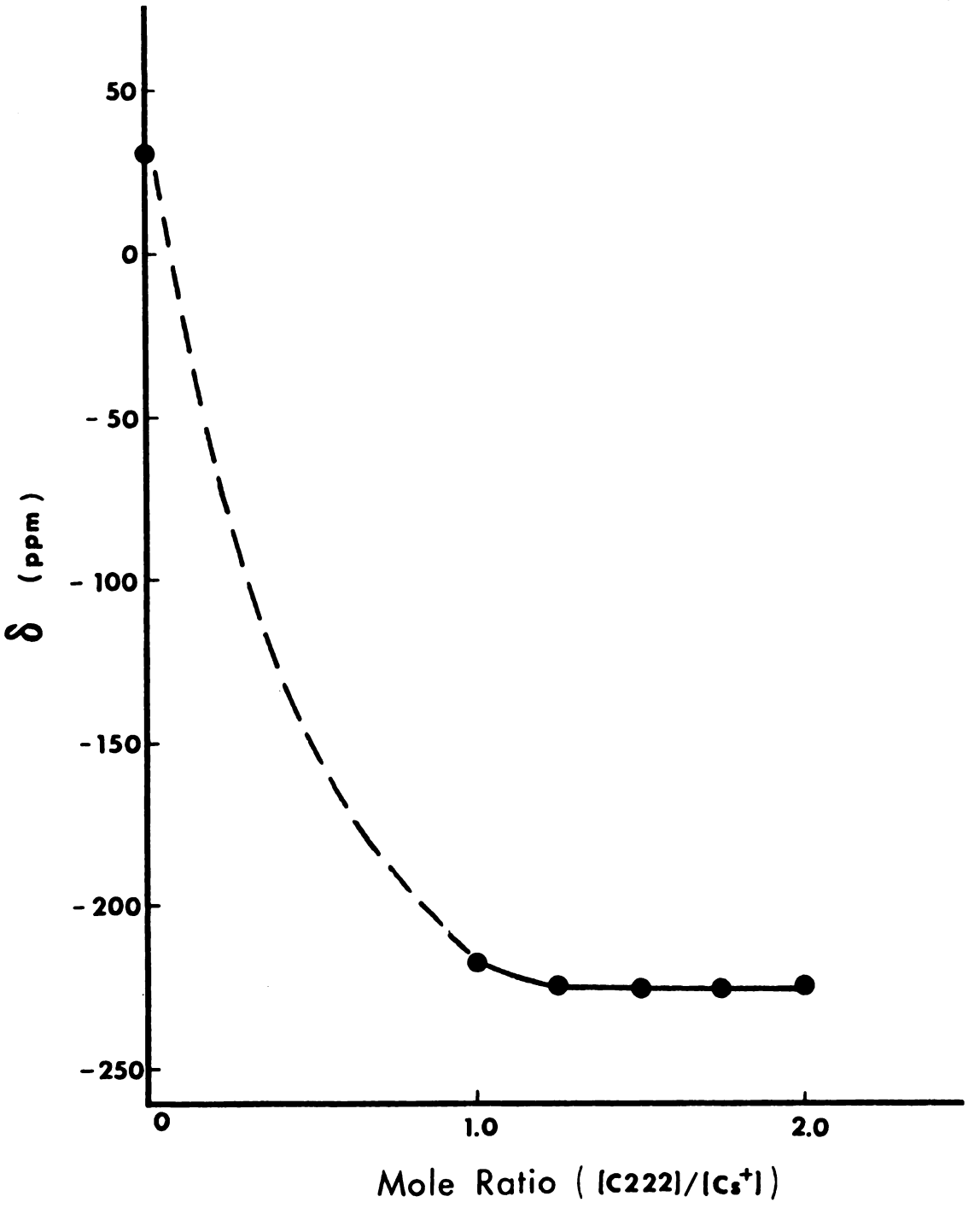

Figure 18. ^{133}Cs Chemical Shifts of $CsB\phi_4$-C222 Cryptate in Pyridine.

CHAPTER V

TEMPERATURE STUDY OF CESIUM COMPLEXES WITH CRYPTANDS C211, C221 AND C222 IN PYRIDINE

INTRODUCTION

Solvent and anion effects of the weak cesium-C211 complex were discussed in Chapter IV together with the effect of the size of ligand cavity of cryptands on the complexation reaction. The strength of complexation is intimately related to the kinetics of the system, which, in this case, involves the rate of exchange of the cesium ion between the solvated and the complexed sites. The temperature dependence of the ^{133}Cs chemical shifts of Cs^+-C211, Cs^+-C221 and Cs^+-C222 cryptates were observed in pyridine solutions. The results discussed here are the preliminary data obtained from the study of temperature effects on the complexation of the cesium ion with these cryptands.

RESULTS AND DISCUSSION

The complexation of cesium tetraphenylborate with C211, C221 and C222 cryptands can be described by the following equilibrium, assuming a 1:1 complex.

$$Cs^+S_x + LS_y = CsL^+S_z + (x+y-z)S$$

where S is the solvent molecule, L is the ligand and x, y and z are the solvation numbers of the cation, ligand and the complex respectively.

Depending on the strength of the complexation interaction, the cesium ion undergoes exchange between the solvated state and the complexed state which can be monitored by ^{133}Cs NMR. At a given temperature, if the mean lifetime at one site is less than $2/(\omega_A-\omega_B)$,

where ω_A and ω_B are the resonance frequencies (in radians per second) of the two different sites, only one signal is observed on the NMR time scale. Furthermore, the signal is broadened by the exchange mechanism especially around the coalescence temperature. The coalescence temperature (T_c) is the temperature at which the random statistical exchange of the cesium nucleus between two (or more) chemical sites is slowed down to the extent that only one averaged signal is observed. If the exchange is slower than 10^7 per second, two signals are observed, corresponding to the free, solvated cesium nucleus and the complexed cesium nucleus.

Since the Cs^+-C211 complex is weak (see Chapter IV), two mole ratios of 2.49 and 6.63 were arbitrarily chosen for this study as the amount of ligand required to reach a state of quantitative complexation is impractical. For the other two ligands which form strong 1:1 complexes with the cesium ion, the samples are prepared such that the exchange region can be observed, i.e. $0<MR<1$. The temperature dependence of the chemical shifts observed are presented in Table 11 in Appendix I and in Figures 19 to 21 together with that of the cesium salt solution. For the cesium-C221 and cesium-C222 cryptates, two separate solutions with a large excess of ligand were also prepared so as to monitor the changes in chemical shift of the complexed cesium ion with changes in temperature. All chemical shifts reported in this study have been corrected for bulk magnetic susceptibility of the solvent and temperature effects on the reference and adjusted to the final reference point of the infinitely dilute concentration of cesium ions in water at 25°C. The error of measurement is $\pm$ 0.3 ppm unless indicated otherwise. The line widths are included in Table 11

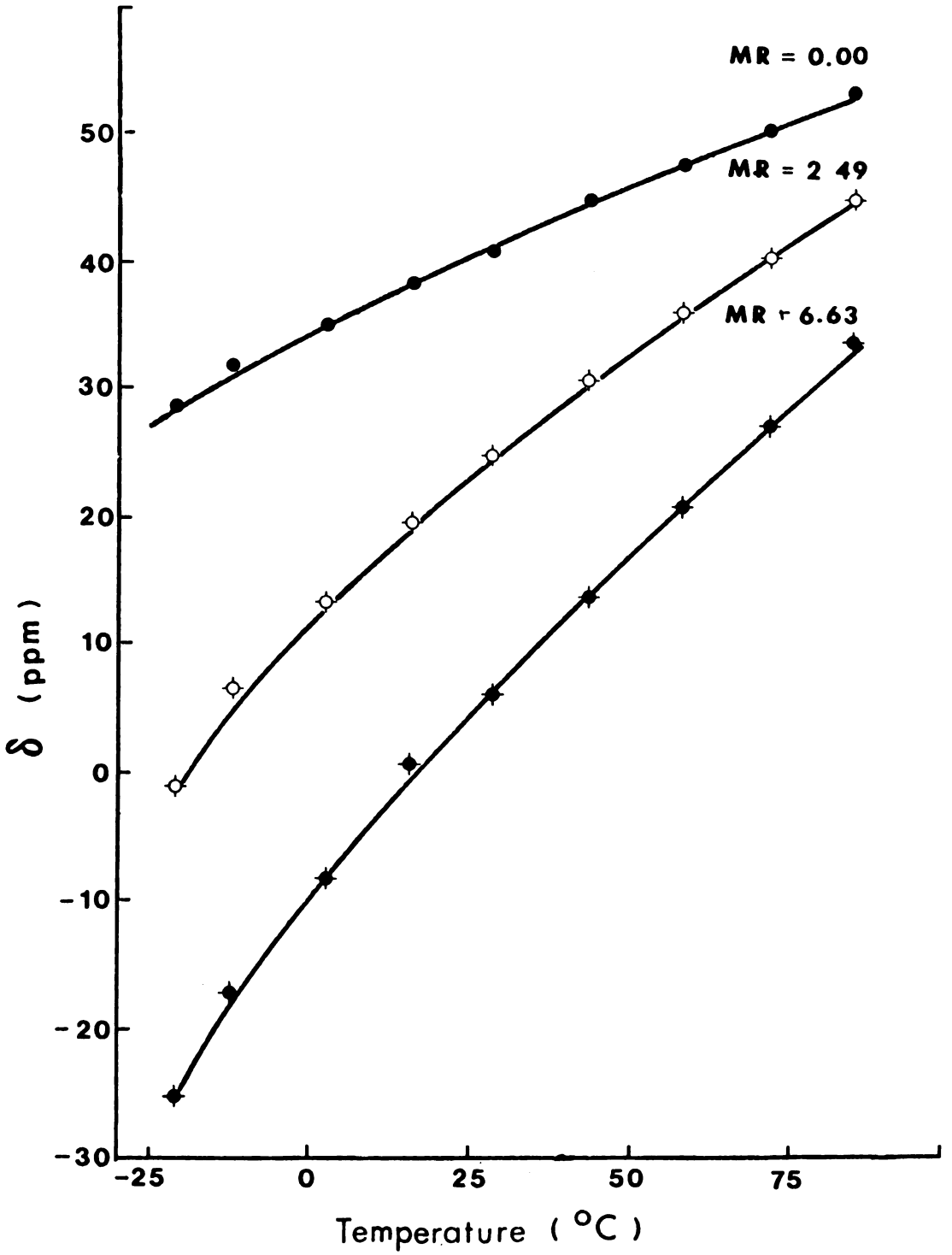

Figure 19. Temperature Dependence of the ^{133}Cs Chemical Shifts of $CsB\phi_4$-C211 Cryptate in Pyridine. $[Cs^+]$ = 0.015 M, MR = $[C211]/[Cs^+]$.

Figure 20A. ^{133}Cs NMR Spectra of $CsB\phi_4$-C221 Cryptate in Pyridine at different Temperatures. (MR = 0.64)

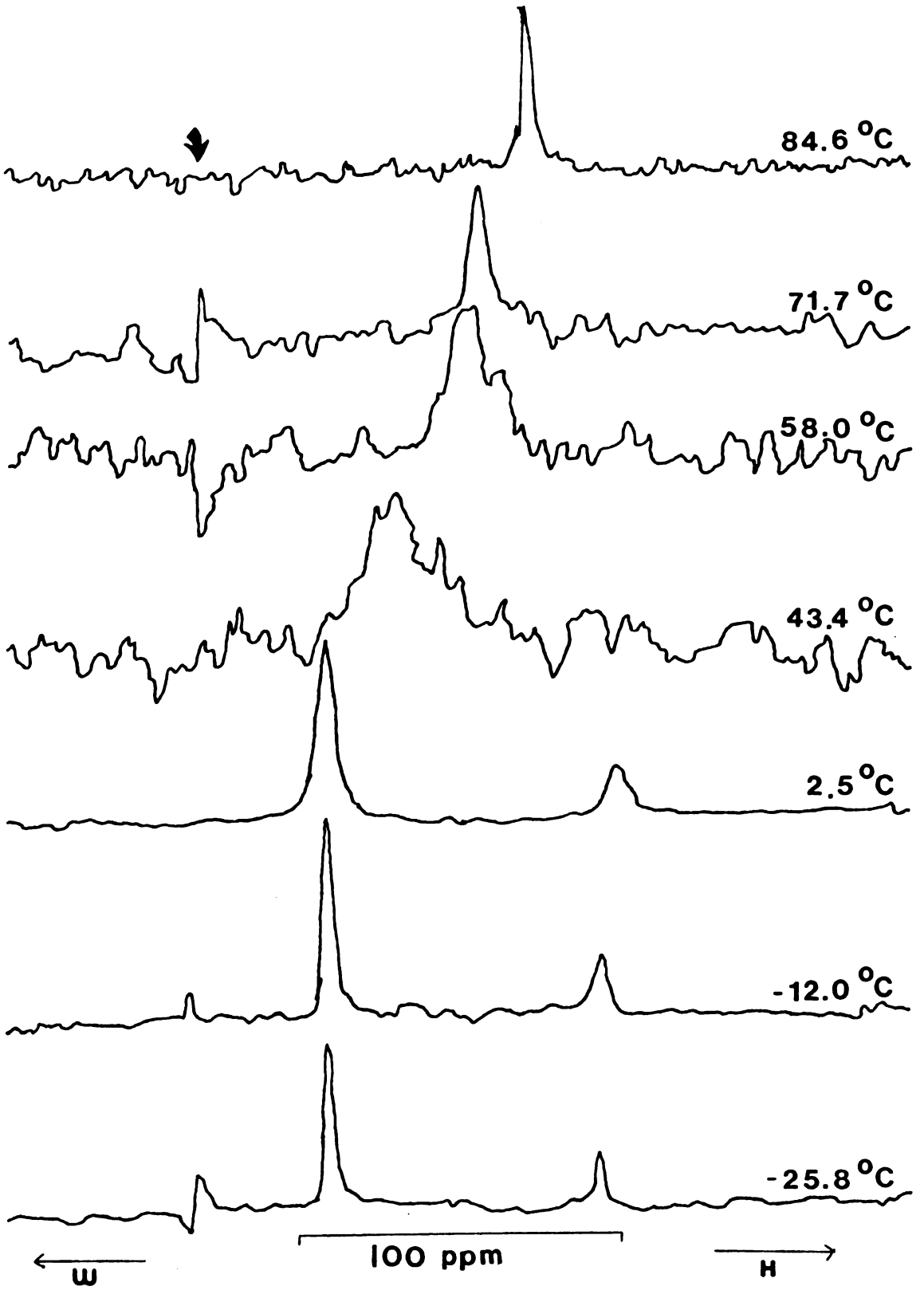

instrumental artifact.

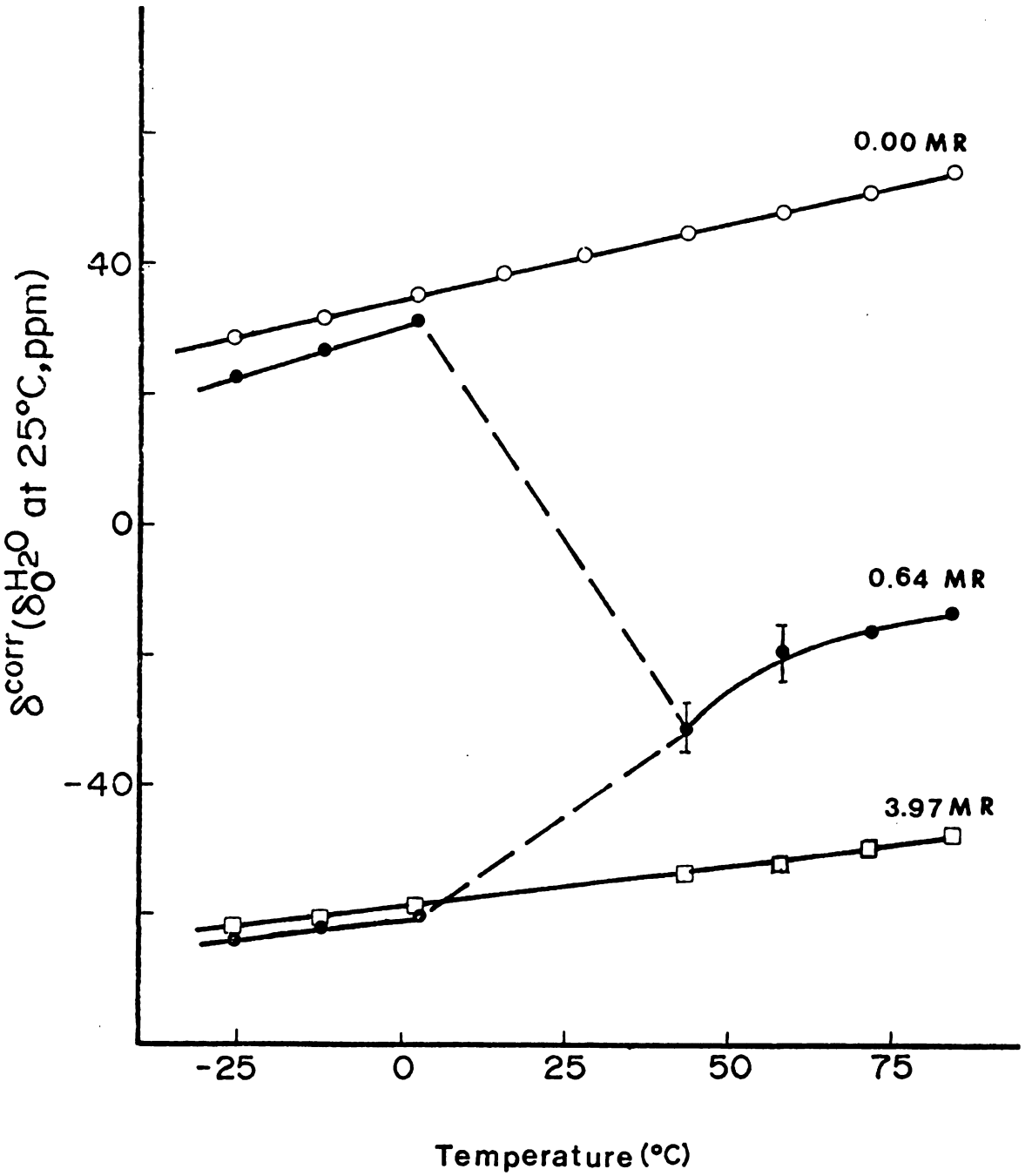

Figure 20B. Temperature Dependence of the ^{133}Cs Chemical Shifts of $CsB\phi_4$-C221 Cryptate in Pyridine. $[Cs^+]$ = 0.015 M, MR = $[C221]/[Cs^+]$.

Figure 21A. ^{133}Cs NMR Spectra of $CsB\phi_4$-C222 Cryptate in Pyridine at different Temperatures. (MR = 0.46)

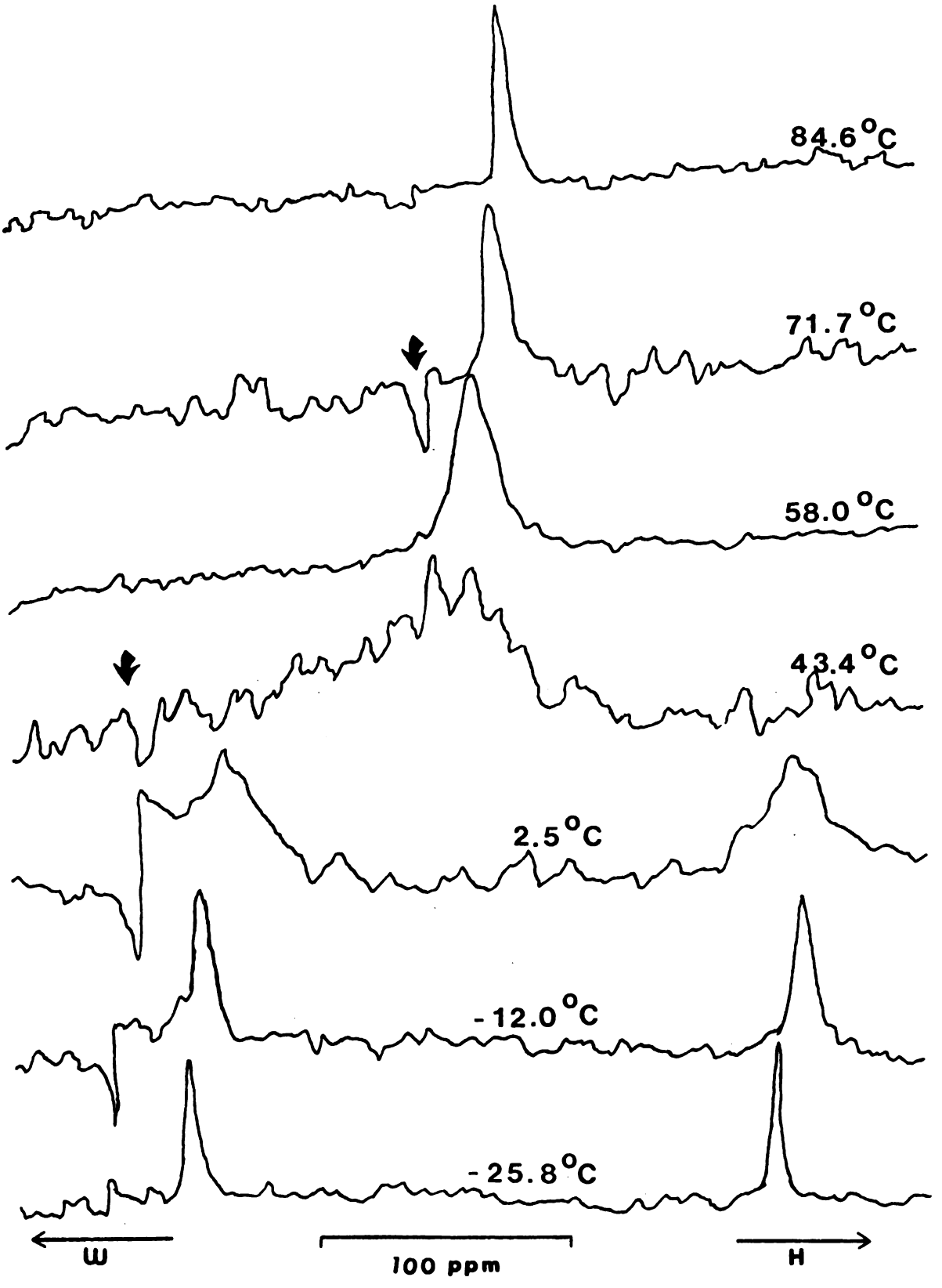

instrumental artifact.

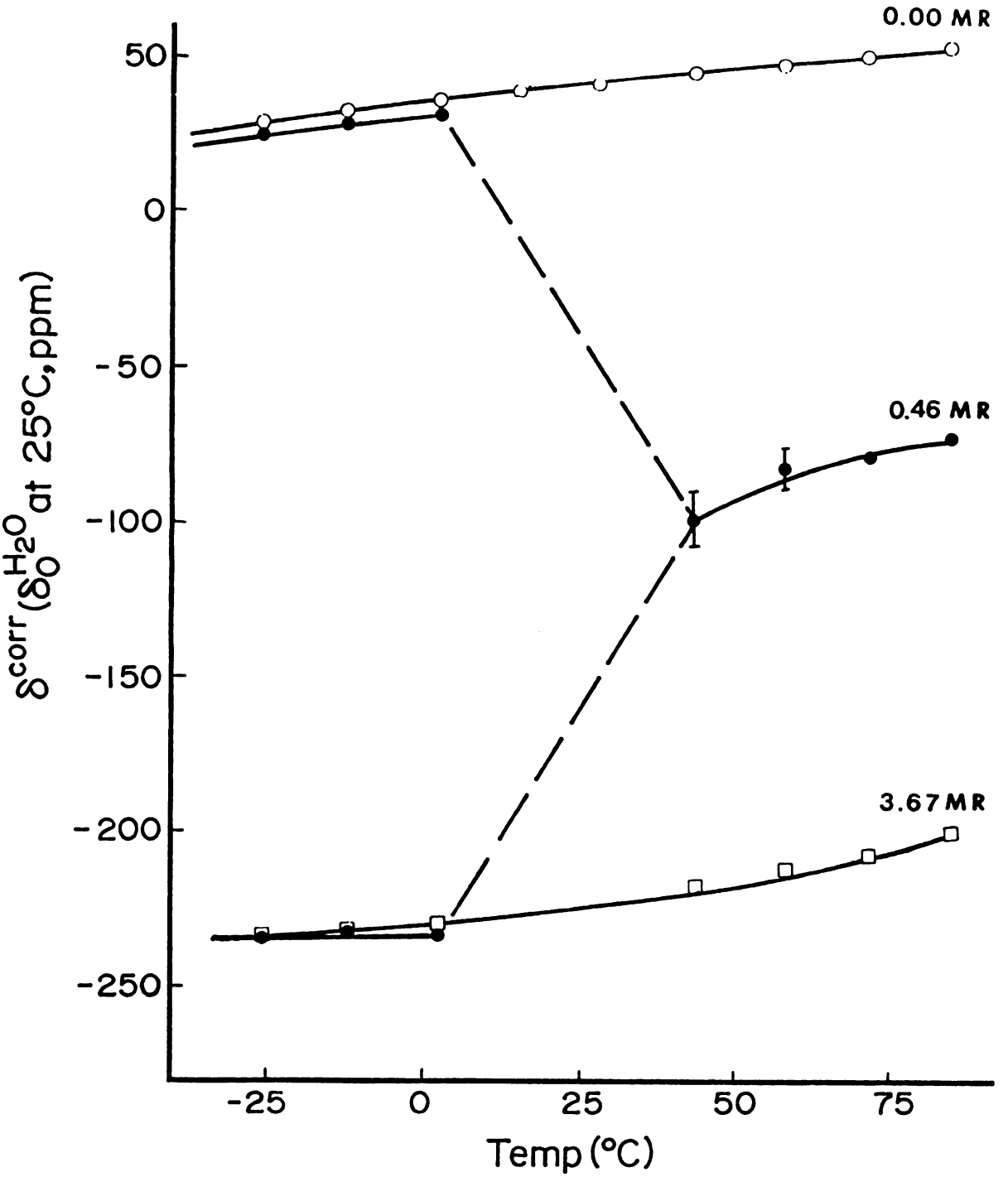

Figure 21B. Temperature Dependence of the ^{133}Cs Chemical Shifts of $CsB\phi_4$- C222 Cryptate in Pyridine. $[Cs^+]$ = 0.015 M, MR = $[C222]/[Cs^+]$.

These values include broadening due to field inhomogeneity, viscosity and the exponential multiplication of the free induction decay signal as discussed in Chapter II. Since only the relative line widths are of interest in this study, no attempt was made to correct them to obtain true line widths.

The ^{133}Cs resonance of 0.015 M $CsB\phi_4$ solution in pyridine move to low field as the temperature is decreased (see Figures 19, 20B and 21B). The two solutions of the Cs^+-C211 cryptate show a linear dependence of the chemical shift with temperature, with slight curvature at low temperatures. The exchange between the complexed cesium ion and the solvated cesium ion is still rapid, even at -25^oC, which is another indication of the weakness of the interaction between the cesium ion and the cryptand C211. At low temperatures, the rates are reduced somewhat and the observed chemical shifts at lower field imply an increase in the averaged electron density at the cesium nucleus, i.e. the lifetime of the cesium complex is increased but is but is still less than 10^{-7} seconds.

The stabilities of the Cs^+-C221 and Cs^+-C222 complexes in pyridine are known to be very much greater than the corresponding C211 complex. The effect of the cavity size of the ligand on the exchange is shown in Figures 20A and 21A. For both of these complexes, the temperature range studied includes the coalescence temperature. In contrast to the much weaker Cs^+-C211 cryptate where only one signal is observed, these two complexes give two kinds of spectra: a single resonance above room temperature and two signals at temperatures below 0^oC. The stronger complexation reaction with the two ligands of larger cavity enable the exchange to be "frozen out",

i.e. the higher stabilities reduce the correlation times (the averaged lifetimes of the environment) in the liquid medium.

In the region of rapid exchange (above T_c), the single resonance observed is a population averaged signal as a result of the fast two site exchange. The chemical shift observed moves to low field as the temperature decreases, which indicates an increase in the population of the complexed site. The exothermic nature of the complex reaction is further substantiated by mole ratio studies of the C221 and C222 cryptates at three temperatures. The data are presented in Table 12 in Appendix I and in Figures 22 and 23. The relative curvatures of the plots are indicative of the strengths of interaction, and for both complexes, the degree of curvature increases as the temperature decreases. This trend implies that the complexation equilibrium is shifted to the right with decreasing temperature,

$$M^+ + L = ML^+$$

with a subsequent increase in the concentration of the complexed cesium and the equilibrium constant.

Extrapolation of the linear portions of the plot intersects at a mole ratio of about 1 at all three temperatures.

The line widths observed for the uncomplexed cesium ion are narrow (about 5 Hz) and are limited by the inhomogeneity of the magnetic field. However, as shown in Figure 24, in the case of the Cs^+-C221 and Cs^+-C222 cryptates, line widths on the order of 500 Hz were observed. This significant broadening is due to the exchange of the cesium ion between the two radically different environments and is especially pronounced as the temperature approaches T_c. The asymptotic increase in line widths could be extrapolated to give an

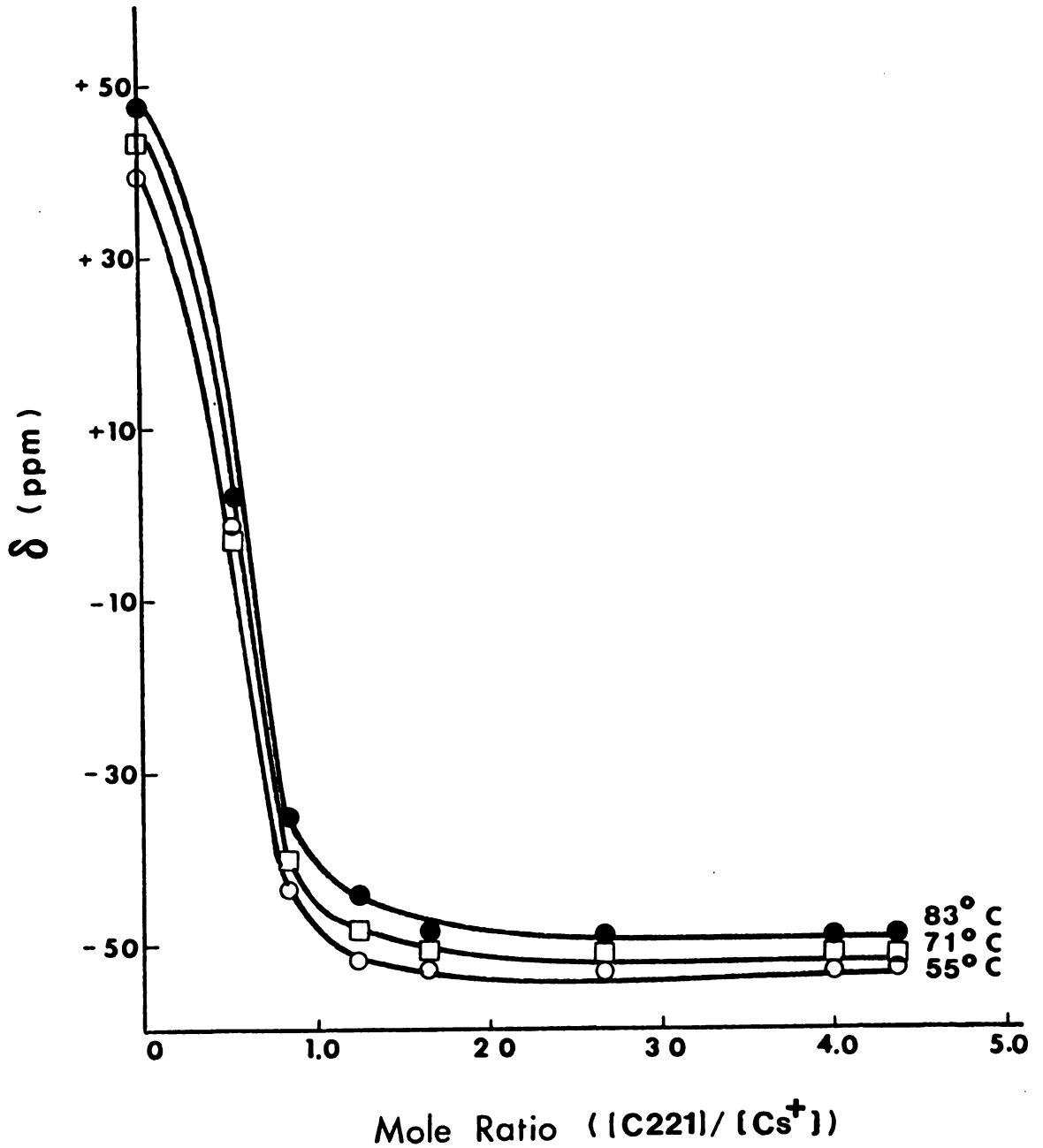

Figure 22. Concentration Dependence of the ^{133}Cs Chemical Shifts of $CsB\phi_4$-C221 Cryptate in Pyridine at Three Temperatures.

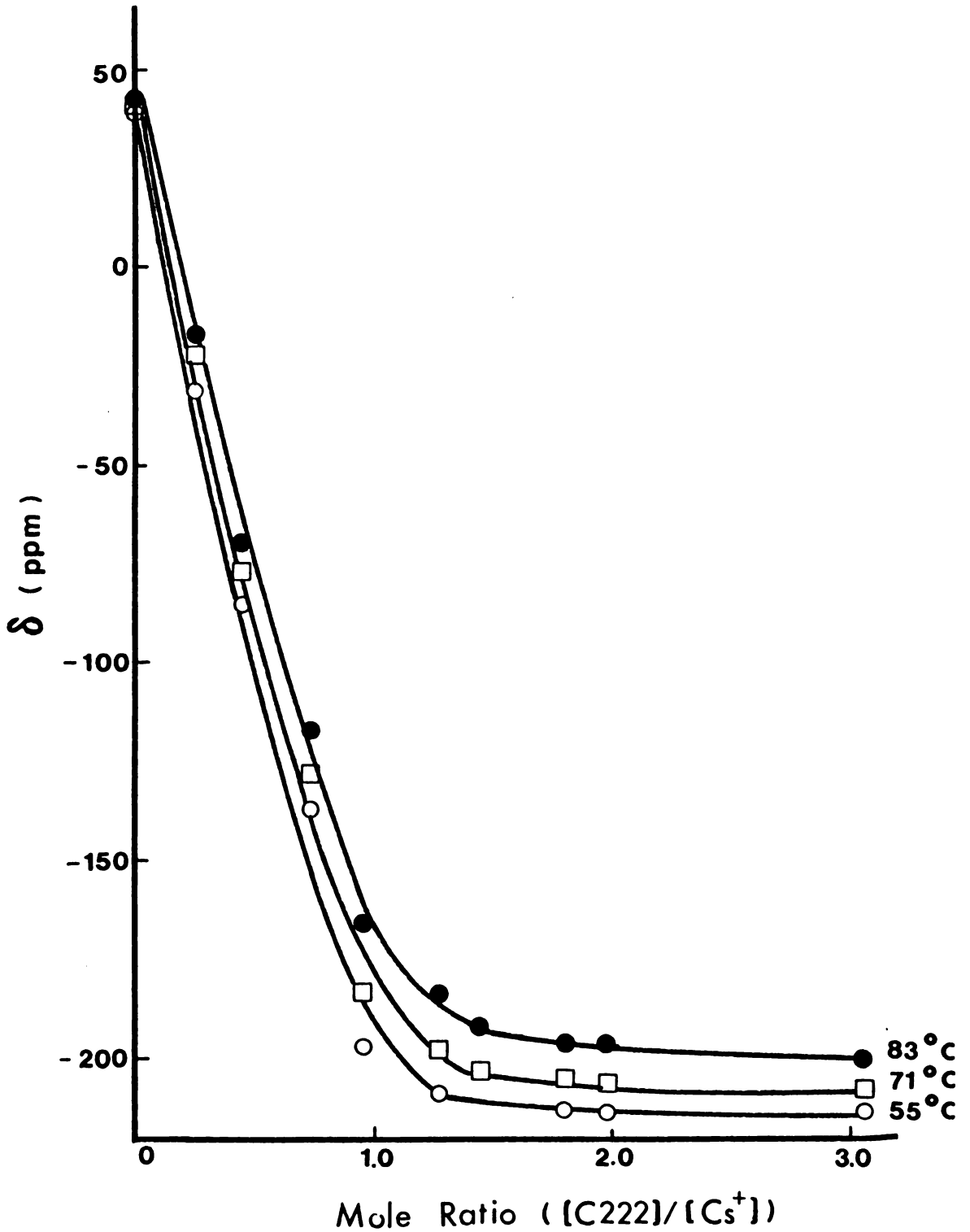

Figure 23. Concentration Dependence of the ^{133}Cs Chemical Shifts of $CsB\phi_4$-C222 Cryptate in Pyridine at Three Temperatures.

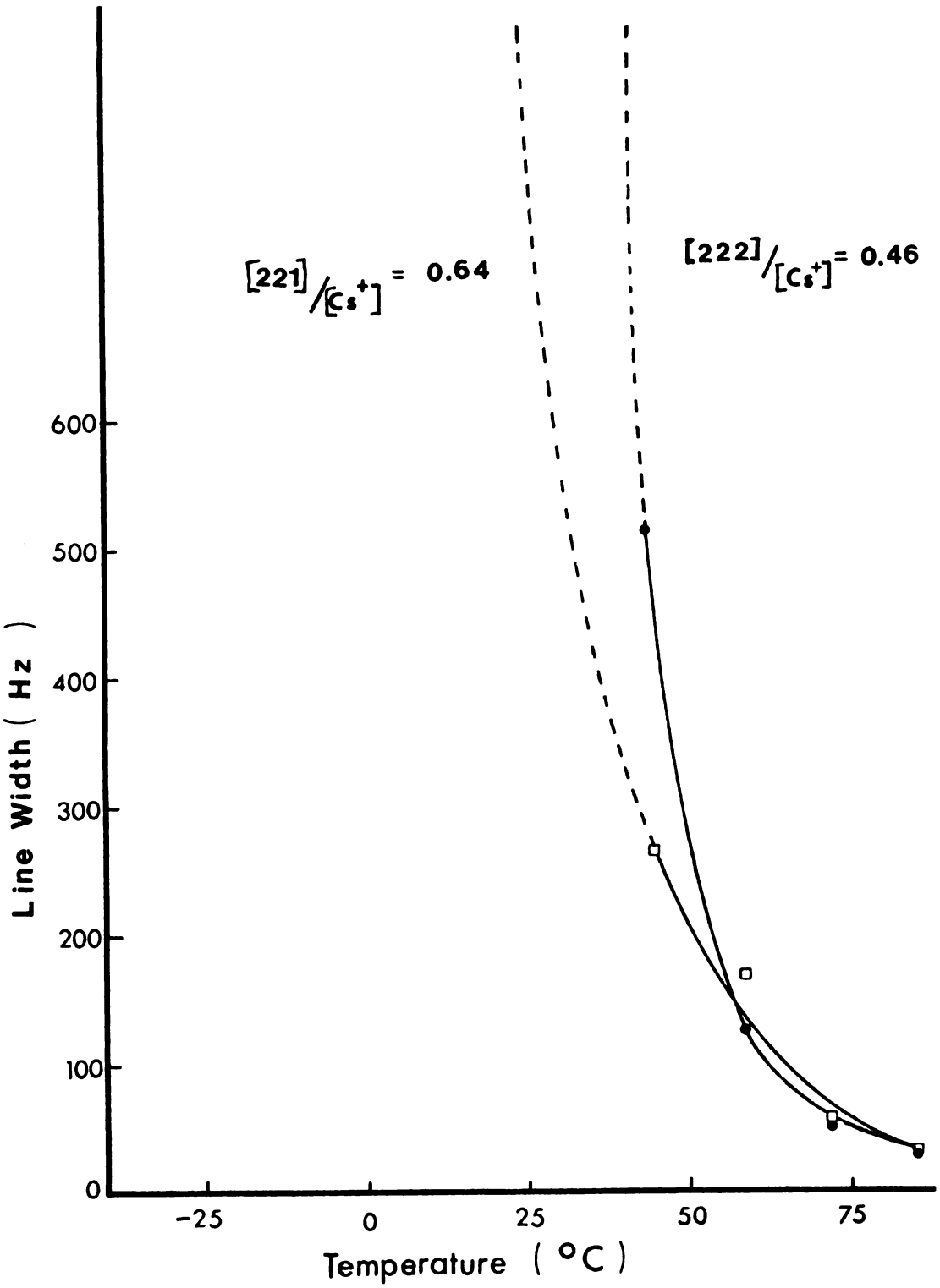

Figure 24. Temperature Dependence of the Uncorrected ^{133}Cs NMR Line Widths of $CsB\phi_4$- C221 and -C222 Cryptates in Pyridine. $[Cs^+]$ = 0.015 M.

estimate of the coalescence temperature. In the case of the Cs^+-C221 complex, coalescence appears to occur around room temperature while the Cs^+-C222 complex has a T_c of about 40°C. This difference in coalescence temperatures seems to indicate that the C222 cryptate is a stronger complex than is the C221 cryptate since a higher temperature is required for the signals to collapse in the rapid limit of exchange.

At the coalescence temperature, the lifetimes τ_M and τ_{ML} are on the same order as $(\omega_M - \omega_{ML})^{-1}$, where τ_M and τ_{ML} are the lifetimes of the free and complexed metal ions respectively, and ω_M and ω_{ML} are the corresponding frequencies in radians per second. Therefore, only one broad signal is observed. At temperatures between 45°C and 2.5°C, no signal was observed for either the C221 or the C222 cryptates. This observation is not surprising if one considers the line broadening that is observed even at 45°C. Extrapolation to lower temperatures would result in very broad lines that are much below the detection limit of the NMR spectrometer. Furthermore, the low cesium ion concentration (0.015 M) would make even signal averaging unrealistically time consuming. In Figures 20B and 21B, this region around coalescence is indicated by the broken lines.

Below T_c, the exchange between the two sites is much slower than 10^7 cycles per second, i.e. $\tau_M, \tau_{ML} > (\omega_M - \omega_{ML})^{-1}$ and two signals emerge: one absorbs at the frequency characteristic of the uncomplexed cesium ion in pyridine and the other at the frequency characteristic of the complexed cesium species, as indicated by the solid lines. The "freezing out" of the exchange is explained by the relaxation model developed quantitatively by McConnell (95) for a nucleus possessing a quadrupole moment: the assumption is made that the nucleus makes

sudden transitions from one site to another. The line widths of both resonances grow progressively narrower as the extreme slow limit of exchange is reached. At the lowest temperature studied, the line widths are on the order of 20 Hz as the exchange is slowed down almost to a standstill.

APPENDICES

APPENDIX I

CESIUM-133 CHEMICAL SHIFT DATA

Table 7. ^{133}Cs Chemical Shifts of Cesium Salt Solutions

$CsB\phi_4$: DMF

Conc. (M)	Chem. Shift (ppm)	Conc. (M)	Chem. Shift (ppm)
0.0009	0.71	0.0704	2.01
0.0019	0.58	0.0803	2.10
0.0039	0.52	0.0897	2.32
0.0053	0.71	0.1002	2.50
0.0059	0.71	0.1254	2.97
0.0069	0.80	0.1499	3.50
0.0087	0.83	0.1755	3.87
0.0101	1.11	0.2004	4.27
0.0196	1.29	0.2256	4.93
0.0294	1.42	0.2493	5.48
0.0395	1.46	0.2752	5.83
0.0504	1.64	0.3001	6.57
0.0608	1.85	0.3368	7.41
		0.3508	7.81

$CsB\phi_4$: DMSO

0.0010	-68.40	0.0500	-67.97
0.0050	-68.40	0.0750	-67.84
0.0080	-68.03	0.1000	-67.54
0.0100	-68.34	0.2500	-66.05
0.0250	-68.16	0.5000	-62.57

Table 7. (continued)

$CsB\phi_4$: Acetone

Conc. (M)	Chem. Shift (ppm)	Conc. (M)	Chem. Shift (ppm)
0.0010	27.84	0.0124	37.08
0.0050	32.05	0.0150	38.57
0.0080	34.29	0.0177	39.68
0.0100	35.53	0.0205	40.68

$CsB\phi_4$: Pyridine

0.0010	- 0.98	0.0080	28.11
0.0020	7.11	0.0090	29.76
0.0030	12.67	0.0100	31.75
0.0040	16.89	0.0107	32.86
0.0050	20.24	0.0124	35.34
0.0060	23.25	0.0153	39.62
0.0070	25.70	0.0168	41.11

CsPi : Acetone

0.0010	25.98	0.0060	24.95
0.0020	25.42	0.0070	24.64
0.0030	25.38	0.0080	24.49
0.0040	25.27	0.0090	24.40
0.0050	24.98	0.0100	23.96

Table 7. (continued)

CsPi : $ForNH_2$

Conc. (M)	Chem. Shift (ppm)	Conc. (M)	Chem. Shift (ppm)
0.0010	2.90	0.0070	2.68
0.0040	2.43	0.0080	2.53
0.0050	2.63	0.0090	2.63
0.0060	2.46	0.0100	2.44
		0.0201	2.69

CsPi : DMF

0.0010	1.49	0.0080	1.01
0.0030	1.25	0.0090	1.08
0.0060	1.18	0.0100	1.00
0.0070	1.13	0.0151	1.03
		0.0363	0.96

CsPi : DMSO

0.0010	- 66.85	0.0050	- 67.94
0.0020	- 67.59	0.0060	- 68.56
0.0030	- 67.75	0.0070	- 68.15
0.0040	- 67.94	0.0080	- 68.16
		0.0090	- 67.88

Table 7. (continued)

$CsClO_4$: $MeNO_2$

Conc. (M)	Chem. Shift (ppm)	Conc. (M)	Chem. Shift (ppm)
0.0010	60.47	0.0060	59.97
0.0020	60.44	0.0070	60.25
0.0030	60.38	0.0080	59.94
0.0040	60.31	0.0090	59.82
0.0050	60.22	0.0100	59.82

CsI : ACN

0.0010	-34.81	0.0060	-39.15
0.0020	-35.96	0.0070	-39.92
0.0030	-36.66	0.0080	-40.46
0.0040	-37.60	0.0090	-41.39
0.0050	-38.36	0.0100	-41.63

CsSCN : H_2O

0.001	-0.03	0.035	-0.53
0.005	-0.16	0.040	-0.59
0.008	-0.16	0.050	-0.65
0.010	-0.22	0.065	-0.72
0.015	-0.28	0.088	-1.09
0.020	-0.35	0.100	-1.27

Table 8. Cesium-133 Chemical Shifts of Cesium-C211 Cryptates in Various Solvents ($[Cs^+]$ = 0.01 M)

$CsB\phi_4$: Acetonitrile

MR*	δ (ppm)	MR*	δ (ppm)
0.00	-24.63	1.87	-28.48
0.45	-25.93	3.00	-30.65
1.00	-26.49	3.92	-32.26
1.50	-28.23	4.89	-33.32
		6.14	-34.38

$CsB\phi_4$: Acetone

0.00	35.56	3.00	27.78
0.24	34.78	3.22	28.58
0.50	33.76	3.54	26.84
0.75	33.39	4.00	26.41
0.99	32.70	5.00	24.73
1.26	31.99	6.00	22.03
1.50	31.50	7.00	20.61
1.74	29.98	8.00	19.96
2.01	29.82	9.00	18.47
2.25	29.54	10.00	17.54
2.46	28.92	15.00	11.64
2.75	27.90	20.18	6.00

Table 8. (continued)

$CsB\phi_4$: PC

MR	δ (ppm)	MR	δ (ppm)
0.00	36.02	2.18	29.94
0.52	34.22	2.98	27.15
1.00	33.05	3.95	25.23
1.56	30.75	5.00	22.68

$CsB\phi_4$: DMSO

0.00	-67.74	3.09	-68.40
1.00	-67.84	4.02	-68.15
2.04	-68.22	6.59	-67.78

$CsB\phi_4$: DMF

0.00	0.81	2.05	0.06
0.55	0.56	3.05	-0.19
1.04	0.31	4.02	-0.56
1.53	0.13	5.13	-0.68

$CsB\phi_4$: Pyridine

0.00	32.92	1.91	22.50
0.59	29.76	3.09	19.65
1.11	26.59	3.85	16.92
1.53	25.29	4.92	13.07

Table 8. (continued)

CsSCN : $MeNO_2$

MR	δ (ppm)	MR	δ (ppm)
0.00	54.83	3.09	28.12
0.52	48.10	3.47	25.14
1.11	42.76	4.09	22.32
1.70	37.61	4.68	19.68
2.15	34.17	5.03	17.68
2.63	30.79	5.62	15.78

CsSCN : Acetone

0.00	17.26	3.02	11.99
1.01	15.68	4.06	9.94
2.01	13.63	6.03	6.81

CsSCN : ACN

0.00	-34.43	3.12	-38.80
1.04	-36.39	3.88	-39.76
2.08	-37.75	5.06	-40.85

CsSCN : DMF

0.00	-0.31	3.19	-1.18
1.04	-0.50	4.09	-1.62
2.11	-0.87	5.13	-1.80

Table 8. (continued)

CsSCN : PC

MR	δ (ppm)	MR	δ (ppm)
0.00	34.45	3.26	26.07
1.14	31.00	4.47	21.91
2.36	25.94	5.31	19.77

CsSCN : DMSO

0.00	-68.09	3.22	-68.09
1.11	-68.06	3.81	-68.09
2.08	-68.09	5.06	-67.91

CsI : ACN

0.00	-41.88	2.95	-45.32
1.01	-43.05	4.06	-46.31
1.98	-44.45	4.96	-47.49

CsI : DMF

0.00	-1.49	3.15	-1.86
1.00	-1.68	4.30	-2.83
1.80	-1.68	4.96	-2.86

CsI : DMSO

0.00	-68.87	3.09	-68.95
1.01	-69.03	4.06	-68.87
2.01	-68.95	5.03	-69.03

Table 8. (continued)

CsI : PC

MR	δ (ppm)	MR	δ (ppm)
0.00	37.89	2.98	24.30
1.07	29.51	3.95	22.04
2.11	26.60	5.55	18.72

CsPi : DMF

0.00	0.96	2.95	0.06
1.04	0.65	3.92	-0.34
2.15	0.22	5.06	-0.93

$CsClO_4$: $MeNO_2$

0.00	59.51	3.95	27.22
1.04	47.44	5.41	20.03
2.05	39.17	8.05	11.24
2.98	32.47	10.26	5.14
		12.10	1.88

CsCl : Methanol

0.00	43.73	3.92	40.85
0.97	43.05	4.99	40.33
2.11	42.24	5.79	39.64
2.95	41.81	6.45	39.80
		7.39	38.56

*MR = $[C211]/[Cs^+]$

Table 9. Cesium-133 Chemical Shifts of $CsB\phi_4$ and C221 Cryptates in Various Solvents

Acetonitrile ($[Cs^+]$ = 0.015 M)

MR*	δppm ($\Delta\nu_{1/2}$ in Hz)		MR	δppm ($\Delta\nu_{1/2}$ in Hz)	
0.00	-21.16	(4)	1.04	-57.84	(8)
0.24	-24.34 ± 2	(100)**	1.14	-59.85	(4)
0.50	-41.94 ± 2	(104)**	1.34	-59.93	(4)
0.78	-51.40	(66)**	1.62	-59.93	(4)
			2.09	-59.78	(5)

Acetone ($[Cs^+]$ = 0.015 M)

0.00	38.34	(5)	0.98	-40.22	(7)
0.28	13.91 ± 3	(230)**	1.12	-44.33	(2)
0.56	- 5.86 ± 3	(200)**	1.22	-44.57	(3)
0.72	-17.88	(70)	1.64	-44.72	(4)
			2.08	-44.56	(4)

DMF ($[Cs^+]$ = 0.015 M)

0.00	1.04	(3)	1.03	-43.86	(5)
0.32	-14.24	(12)	1.13	-46.41	(5)
0.61	-28.58	(10)**	1.34	-48.52	(4)
0.81	-37.74	(7)**	1.73	-50.38	(3)
0.89	-40.37	(5)	2.03	-50.84	(4)
			2.58	-51.31	(3)

Table 9. (continued)

PC ($[Cs^+]$ = 0.012 M)

MR	δ ppm ($\Delta\nu_{1/2}$ in Hz)		MR	δ ppm ($\Delta\nu_{1/2}$ in Hz)	
0.00	36.38	(3)	1.00	-40.77	(16)
0.25	26.75 ± 5	(390)**	1.18	-44.03	(5)
0.73	-21.85 ± 2.5	(237)**	1.35	-44.19	(6)
0.90	-40.24	(16)	2.11	-44.19	(5)

DMSO ($[Cs^+]$ = 0.015 M)

0.00	-67.85	(4)	1.77	-71.57	(4)
0.30	-68.77	(4)	2.05	-71.69	(4)
0.70	-69.95	(6)	2.23	-71.67	(4)
1.10	-70.89	(6)	2.73	-71.81	(4)
1.24	-71.25	(4)	3.01	-71.94	(3)
1.51	-71.50	(3)	3.65	-71.81	(4)

Pyridine ($[Cs^+]$ = 0.010 M)

0.00	31.74	(8)	1.23	-57.59	(11)**
0.54	---	---	1.65	-57.90	(3)
0.84	-51.07	(61)**	2.68	-57.90	(2)
			4.00	-57.90	(4)

*MR = $[C221]/[Cs^+]$

**Free induction decay signal was multiplied by large exponential factor to optimize signal-to-noise ratio.

Table 10. ^{133}Cs Chemical Shifts of $CsB\phi_4$ and C222 Cryptate in Pyridine ($[Cs^+]$ = 0.01 M)

MR*	δ (ppm)	$\Delta\nu_{1/2}$ (Hz)
0.0	30.81	3
0.25	---	--
0.50	---	--
0.75	---	--
1.00	-217.33	15
1.25	-223.85	14
1.50	-224.47	7
1.75	-224.15	12
2.0	-224.15	9

*MR = $[C222]/[Cs^+]$

Table 11. ^{133}Cs Chemical Shifts of $CsB\phi_4$ and Cryptands in Pyridine at Different Temperatures ($[Cs^+]$ = 0.015 M, MR = [cryptand]/$[Cs^+]$)

$CsB\phi_4$-211 Cryptate

Temp.	MR = 0.00 δppm ($\Delta\nu_{1/2}$ Hz)		MR = 2.49 δppm ($\Delta\nu_{1/2}$ Hz)		MR = 6.63 δppm ($\Delta\nu_{1/2}$ Hz)	
84.6	53.53	(3)	45.15	(24)	33.67	(27)
71.7	50.42	(4)	40.50	(17)	27.16	(24)
58.0	47.63	(2)	36.15	(15)	20.96	(22)
43.4	44.84	(2)	30.88	(15)	13.82	(20)
28.2	41.12	(2)	24.99	(15)	6.07	(17)
15.7	38.64	(2)	19.71	(17)	0.76	(17)
2.5	35.22	(2)	13.51	(17)	- 8.20	(20)
-12.0	31.81	(2)	6.69	(17)	-16.89	(27)
-25.8	28.71	(4)	- 1.07	(24)	-25.26	(29)

$CsB\phi_4$-221 Cryptate

	MR = 0.64				MR = 3.97	
84.6	-13.78	(32)			-47.90	(12)
71.7	-16.27	(54)			-50.08	(12)
58.0	-19.06 ± 2	(173)*			-51.94	(12)
43.4	-31.47 ± 2	(271)*			-53.49	(10)
2.5	-59.69	(46)*	31.19	(81)*	-58.76	(22)
-12.0	-61.86	(20)	26.85	(29)	-60.31	(5)
-25.8	-63.41	(15)	22.82	(17)	-61.55	(12)

Table 11. (continued)

$CsB\phi_4$-222 Cryptate

Temp.	MR = 0.46 δ ppm ($\Delta\nu_{1/2}$ Hz)				MR = 3.67 δ ppm ($\Delta\nu_{1/2}$ Hz)	
84.6	-70.24	(34)			-200.20	(12)
71.7	-78.61	(59)			-207.03	(15)
58.0	-82.65 ± 1	(134)			-212.61	(15)
43.4	-98.77 ± 5	(515)*			-217.57	(17)
2.5	-232.77	(400)*	31.50	(183)*	-229.05	(15)
-12.0	-231.53	(63)	28.71	(46)	-231.22	(17)
-25.8	-233.08	(29)	25.30	(22)	-232.77	(20)

*Free induction decay signal was multiplied by large exponential factor to optimize signal-to-noise ratio.

Table 12. Cesium-133 Chemical Shifts of Cesium-C221 and Cesium-C222 Cryptates in Pyridine at Three Temperatures ($[Cs^+]$ = 0.01 M)

$CsB\phi_4$-C221 in Pyridine

MR*	83.5° C	70.0° C	55.0° C
0.00	47.52	43.52	39.16
0.54	2.23	- 3.01 ± 3	- 1.33 ± 5
0.85	-35.30	-39.92	-43.65
1.23	-44.29	-48.30	-51.71
1.65	-48.33	-50.78	-52.95
2.68	-48.64	-50.78	-53.26
4.00	-48.95	-51.09	-53.26
4.36	-48.95	-51.09	-53.26

$CsB\phi_4$-C222 in Pyridine

0.00	43.49	42.28	38.54
0.25	- 16.68	- 21.93	- 32.80 ± 3
0.45	- 70.10	- 76.83 ± 2	- 85.22 ± 2
0.72	-117.50	-128.01	-136.71
0.96	-166.82	-182.60	-197.19
1.27	-183.57	-197.49	-208.98
1.46	-192.26	-203.39	-212.08
1.81	-196.29	-205.25	-213.01
1.97	-196.91	-205.87	-213.32
3.05	-199.70	-206.80	-213.01

*MR = $[Ligand]/[Cs^+]$

APPENDIX II

DETERMINATION OF COMPLEX FORMATION CONSTANT WITH ION PAIR FORMATION BY THE NMR METHOD

DETERMINATION OF COMPLEX FORMATION CONSTANT WITH ION PAIR FORMATION BY THE NMR METHOD

Definition of symbols,

$[M]$ = cation

$[A]$ = anion

$[L]$ = ligand

$[MA]$ = ion pair

$[ML]$ = metal complex

C_M = analytical concentration of metal ion

C_L = analytical concentration of ligand

K_{ip} = ion pair equilibrium constant

K^f = formation constant of complex

Ion pair equilibrium,

$$[M] + [A] \overset{K_{ip}}{\rightleftharpoons} [MA]$$

$$K_{ip} = \frac{[MA]}{[M][A]} \tag{15}$$

Complexation equilibrium,

$$[M] + [L] \overset{K^f}{\rightleftharpoons} [ML]$$

$$K^f = \frac{[ML]}{[M][L]} \tag{16}$$

$$C_L = [M] + [L] \tag{17}$$

$$C_M = [ML] + [M] + [MA] \tag{18}$$

$$C_M = [MA] + [A] \tag{19}$$

From (15),

$$[MA] = K_{ip}[M][A] \tag{20}$$

From (16),

$$[ML] = K^f[M][L] \tag{21}$$

Substitute in (13),

$$C_L = K^f[M][L] + [L] = [L](K^f[M] + 1)$$

$$\therefore [L] = \frac{C_L}{K^f[M] + 1} \tag{22}$$

Substitute in (18),

$$C_M = K^f[M][L] + [M] + K_{ip}[M][A] \tag{23}$$

Substitute in (19),

$$C_M = [A] + K_{ip}[M][A] = [A](1 + K_{ip}[M])$$

$$\therefore [A] = \frac{C_M}{1 + K_{ip}[M]} \tag{24}$$

Substitute (22) and (24) in (23),

$$C_M = \frac{K^f[M]C_L}{K^f[M] + 1} + [M] + \frac{K_{ip}[M]C_M}{1 + K_{ip}[M]} \tag{25}$$

Multiply (25) across by $(1 + K^f[M])(1 + K_{ip}[M])$,

$$C_M(1 + K^f[M])(1 + K_{ip}[M]) = K^f C_L[M](1 + K_{ip}[M])$$

$$+ [M](1 + K^f[M])(1 + K_{ip}[M]) + K_{ip}C_M[M](1 + K^f[M]) \tag{26}$$

$$C_M + K_{ip}C_M[M] + K^fC_M[M] + K^fK_{ip}C_M[M]^2$$

$$= K^fC_L[M] + K^fK_{ip}C_L[M]^2 + [M] + K_{ip}[M]^2$$

$$+ K^f[M]^2 + K^fK_{ip}[M]^3 + K_{ip}C_M[M] + K^fK_{ip}C_M[M]^2 \qquad (27)$$

Collecting terms,

$$K^fK_{ip}[M]^3 + (K^fK_{ip}C_L + K_{ip} + K^f)[M]^2$$

$$+ (K^fC_L + 1 - K^fC_M)[M] - C_M = 0 \qquad (28)$$

$$[M]^3 + \frac{(K^fK_{ip}C_L + K_{ip} + K^f)}{K^fK_{ip}}[M]^2$$

$$+ \frac{(K^fC_L + 1 - K^fC_M)}{K^fK_{ip}}[M] - \frac{C_M}{K^fK_{ip}} = 0 \qquad (29)$$

Solution to cubic equation,

$$y^3 + py^2 + qy + r = 0$$

$$p = \frac{(K^fK_{ip}C_L + K_{ip} + K^f)}{K^fK_{ip}}$$

$$q = \frac{(K^fC_L + 1 - K^fC_M)}{K^fK_{ip}}$$

$$r = \frac{-C_M}{K^fK_{ip}}$$

$$y = x - \frac{p}{3}$$

$$x^3 + ax + b = 0$$

$$a = (3q - p^2)/3$$

$$b = (2p^3 - 9pq + 27r)/27$$

$$A = \sqrt[3]{-\frac{b}{2} + \sqrt{\frac{b^2}{4} + \frac{a^3}{27}}}$$

$$B = \sqrt[3]{-\frac{b}{2} - \sqrt{\frac{b^2}{4} + \frac{a^3}{27}}}$$

Case I $\quad \frac{b^2}{4} + \frac{a^3}{27} > 0 \rightarrow 1$ real root

II $\quad \frac{b^2}{4} + \frac{a^3}{27} = 0 \rightarrow 3$ real roots

III $\quad \frac{b^2}{4} + \frac{a^3}{27} < 0 \rightarrow 3$ real roots

Case I, $x = A + B$

Case II and III, use trigonometric form

$$\text{Cos}\phi = -\frac{b}{2} \div \sqrt{(-\frac{a^3}{27})}$$

$$x = 2\sqrt{-\frac{a}{3}} \ \text{Cos} \ \frac{\phi}{3}$$

$$2\sqrt{-\frac{a}{3}} \ \text{Cos} \ (\frac{\phi}{3} + 120^\circ)$$

$$2\sqrt{-\frac{a}{3}} \ \text{Cos} \ (\frac{\phi}{3} + 240^\circ)$$

Now, solve for [M] in (29).

Then substitute in following equations,

$$[ML] = \frac{K^f C_L [M]}{K^f [M] + 1} \tag{30}$$

$$[MA] = \frac{K_{ip} C_M [M]}{K_{ip} [M] + 1} \tag{31}$$

$$\delta_{obs} = x_M \delta_M + x_{ML} \delta_{ML} + x_{MA} \delta_{MA} \tag{32}$$

$$\delta_{obs} = \frac{[M]}{C_L} \delta_M + \frac{[ML]}{C_M} \delta_{ML} + \frac{[ML]}{C_M} \delta_{MA} \tag{33}$$

Use final form of δ_{obs} in EQN subroutine.

Coding symbols in EQN,

a = AA	p = PP
b = BB	q = QQ
A = AAA	r = RR
B = BBB	ϕ = FE
y = R	Cos ϕ = CFE

CONST(1) = Kip

CONST(2) = C_M

CONST(3) = δ_{ip}

CONST(4) = δ_M

U(1) = δ_{ML}	XX(1) = C_L
U(2) = K_c^f	XX(2) = δ_{obs}

```
      SUBROUTINE EQN                                                    EQN 1281
      COMMON KOUNT,ITAPE,JTAPE,IWT,LAB,XINCR,NOPT,NOVAR,NOUNK,X,U,ITMAX,EQN 1282
     1WTX,TEST,I,AV,RESID,IAR,EPS,ITYP,XX,RXTYP,DXII,EQP,EQ,EU,P,ZL,TO,EEQN 1283
     2IGVAL,XST,T,DT,L,M,JJJ,Y,DY,VECT,NCST,CONST                       EQN 1284
      DIMENSION X(4,100), U(20), WTX(4,100), XX(4), EQP(100), EQ(100), EEQN 1285
     1U(100), P(20,21), VECT(20,21), ZL(100), TO(20), EIGVAL(20), XST(10EQN 1286
     20), Y(10), DY(10), CONST(16)                                      EQN 1287
      GO TO (2,3,4,5,1), ITYP                                           EQN 1295
    1 CONTINUE                                                          EQN 1296
      ITAPE=60                                                          EQN 1300
      JTAPE=61                                                          EQN 1302
      WRITE (JTAPE,6)                                                   EQN 1303
    6 FORMAT(* FORMATION CONSTANT WITH ION PAIRING*/////)
      NOUNK=2
      NOVAR=2                                                           EQN 1319
      RETURN                                                            EQN 1320
    2 CONTINUE                                                          EQN 1321
CDEFINITIONS OF THE TERMS
C       CONST(1)   =  ION PAIR FORMATION CONSTANT
C       CONST(2)    =    TOTAL CONC. OF METAL
C       CONST(3)    =    CHEM. SHIFT OF ION PAIR
C       CONST(4)    =    CHEM. SHIFT OF METAL
C       U(1)     =    CHEM. SHIFT OF COMPLEXED METAL
C       U(2)     =    FORMATION CONSTANT OF COMPLEX
C       XX(1)    =     TOTAL CONC. OF LIGAND
C       XX(2)    =     OBSERVED CHEM. SHIFT
      CUBR=1./3.
CSETTING THE COEFFICIENTS OF THE TERMS
      PP=XX(1)+(1./U(2))+(1./CONST(1))
      QQ=(1./(U(2)*CONST(1)))+(XX(1)-CONST(2))/CONST(1)
      RR=-CONST(2)/(U(2)*CONST(1))
      AA=(3.*QQ-PP**2)/3.
      BB=(2.*(PP**3)-9.*PP*QQ+27.*RR)/27.
CCHECK POINT FOR WHICH FORM OF THE SOLUTION IS TO BE USED
      TEST=(BB**2)/4.+(AA**3)/27.
      IF (TEST)11,11,12
CTHE ALGEBRIAC FORM IS USED HERE
   11 TA=(-BB/2.+SQRT(TEST))
      AAA=(ABS(TA))**CUBR
      TB=(-BB/2.-SQRT(TEST))
      BBB=(ABS(TB))**CUBR
CCHECKING THE SIGN OF THE CUBEROOT TERMS
      IF (TA)17,17,18
   17 AAA=-AAA
   18 IF (TB)19,19,25
   19 BBB=-BBB
   25 RR=AAA+BBB
      R=RR-(PP/3.)
      GO TO 30
CTHE TRIGONOMETRIC FORM OF THE SOLUTION IS USED HERE
   12 FLAG=0.
      RAD=2.*ACOS(-1.)
      ANGLE=RAD/3.
      FFE=(-BB/2.)/(SQRT(ABS((-AA**3)/27.)))
CCHECK FOR VALIDITY OF COSINE TERM
      IF((FFE.LT.-1.).OR.(FFE.GT.1.)) GO TO 20
      FE=RAD-ACOS(FFE)
   14 RR=2.*(SQRT(ABS(-AA/3.)))*COS(FE/3.+ANGLE*FLAG)
      R=RR-(PP/3.)
CCHECK FOR VALIDITY OF THE CALCULATED METAL CONC
      IF(R)13,13,30
   13 WRITE(JTAPE,22)
   22 FORMAT(* COSINE OF FFE OUTSIDE OF +1 AND -1*)
      STOP
CGO BACK AND FIND ANOTHER ROOT
   20 FLAG=FLAG+1.
      IF(3.-FLAG)15,15,14
   15 WRITE(JTAPE,21)
   21 FORMAT( * ALL THREE ROOTS FLUNKED*)
      STOP
CSUBSTITUTE CALCULATED METAL CONC. IN ORIGINAL EQUATION
   30 DELTA=(R*CONST(4)+(U(2)*R*XX(1)*U(1))/(1.+U(2)*R)+(CONST(1)*R*CONS
     1T(2)*CONST(3))/(1.+CONST(1)*R))/CONST(2)
      RESID=DELTA-XX(2)
    3 CONTINUE                                                          EQN 1334
    4 CONTINUE                                                          EQN 1342
    5 CONTINUE                                                          EQN 1348
      RETURN
      END
```

APPENDIX III

SUGGESTIONS FOR FUTURE WORK

SUGGESTIONS FOR FUTURE WORK

The results of this study have shown that ^{133}Cs NMR can be used advantageously as a powerful technique to study interactions in solution. At the same time, this investigation emphasizes the complexities of solvent-solute and solute-solute interactions. The following suggestions highlights the key areas for further work.

The $CsB\phi_4$ ion pair appears to be highly associated in pyridine, ACN, PC and acetone. The structural and chemical orientation of the anion to the cesium cation remains unknown. One would expect that perturbations at the phenyl rings would be reflected in the decoupled ^{13}C chemical shifts. Functional group spectroscopy could also prove to be illuminating.

Weak complexes in solution are difficult to monitor as shown by the Cs^+-C211 cryptates. Keeping in mind that anion, solvent and ligand are all keen competitors for the cation, one can attempt to differentiate mathematically the three interactions.

$$\delta_{obsd} = x_M \delta_M + x_{ML} \delta_{ML} + x_{MA} \delta_{MA}$$

The three terms in the above expression are in effect, the cation-solvent, cation-ligand and cation-anion interactions. Assuming an ideal situation whereby one can determine the chemical shift values of the solvated, complexed and ion paired cesium ion, it is possible to conceive of a plot such as in Figure 25. The cesium ion concentration is kept constant and curves A and C are mole ratio plots where "anion" and ligand respectively, are added to the solution. The former can be approximated by using a large, inert counterion such as the tetra-

alkylammonium cation. Curve B is the sum of curves A and C. Using raw data from an experiment, one can breakdown the observed chemical shift into into the components in Figure 25 and obtain some insight into the phenomena occuring in solution. If the anion is involved in the complex, the contribution from curve A, the cation-anion interaction, would be fairly constant. However, should the complexed state consist of only the solvated cesium ion and ligand, anions would be "released" into the bulk medium. Finally, using data simulation, the process can be reversed to obtain a better understanding of the relationship between the various interactions.

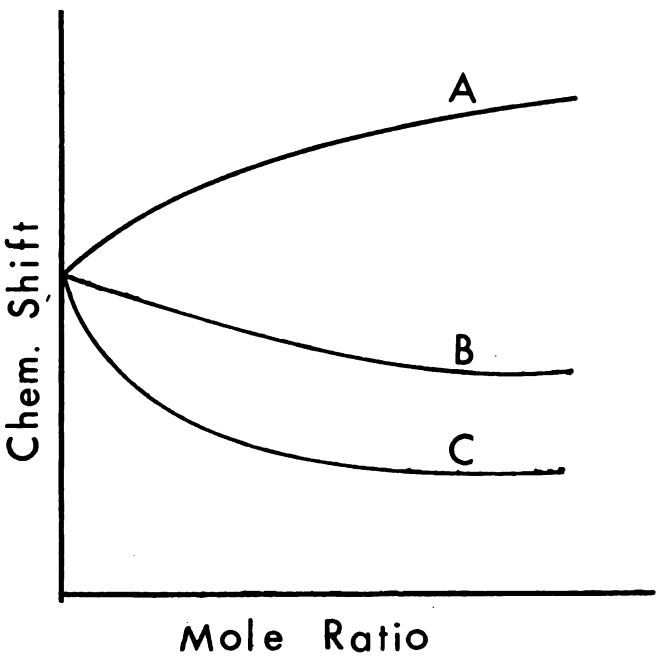

Figure 25. Sample Plot.

The temperature study of the cesium ion with cryptand C211 produced some very interesting data. In Figure 26, the uncorrected line widths are plotted against temperature for the two solutions of the C211 cryptate. There appears to be a minimum in both of these curves. In the event of a 1:1 complex where only one mechanism is predominant, the line width should decrease as the temperature increases in the rapid limit of exchange. The unexpected and inexplicable increase in line width beyond 25°C seems to indicate that more than one relaxation mechanism is present. It also introduces the possibility of a concentration dependent relaxation phenomenon and second order kinetics. Furthermore, Lehn has suggested the possibility of 2:1 complexes (53) of cesium cryptates. However, in this present study, we have not observed evidence at ambient probe temperature, to support the theory of a 2:1 complex. It would be interesting and informative to obtain mole ratio plots of the Cs^+-C211 complex at various temperatures and extend the high temperature limit to see if the line widths do reach a limiting value.

The temperature study of the cryptates can be readily extended to obtain kinetic information. Bloch's equations can be applied to the exchange between the complexed and free cesium ion and the rate of release of cesium ion from the complex can be determined together with the activation energy.

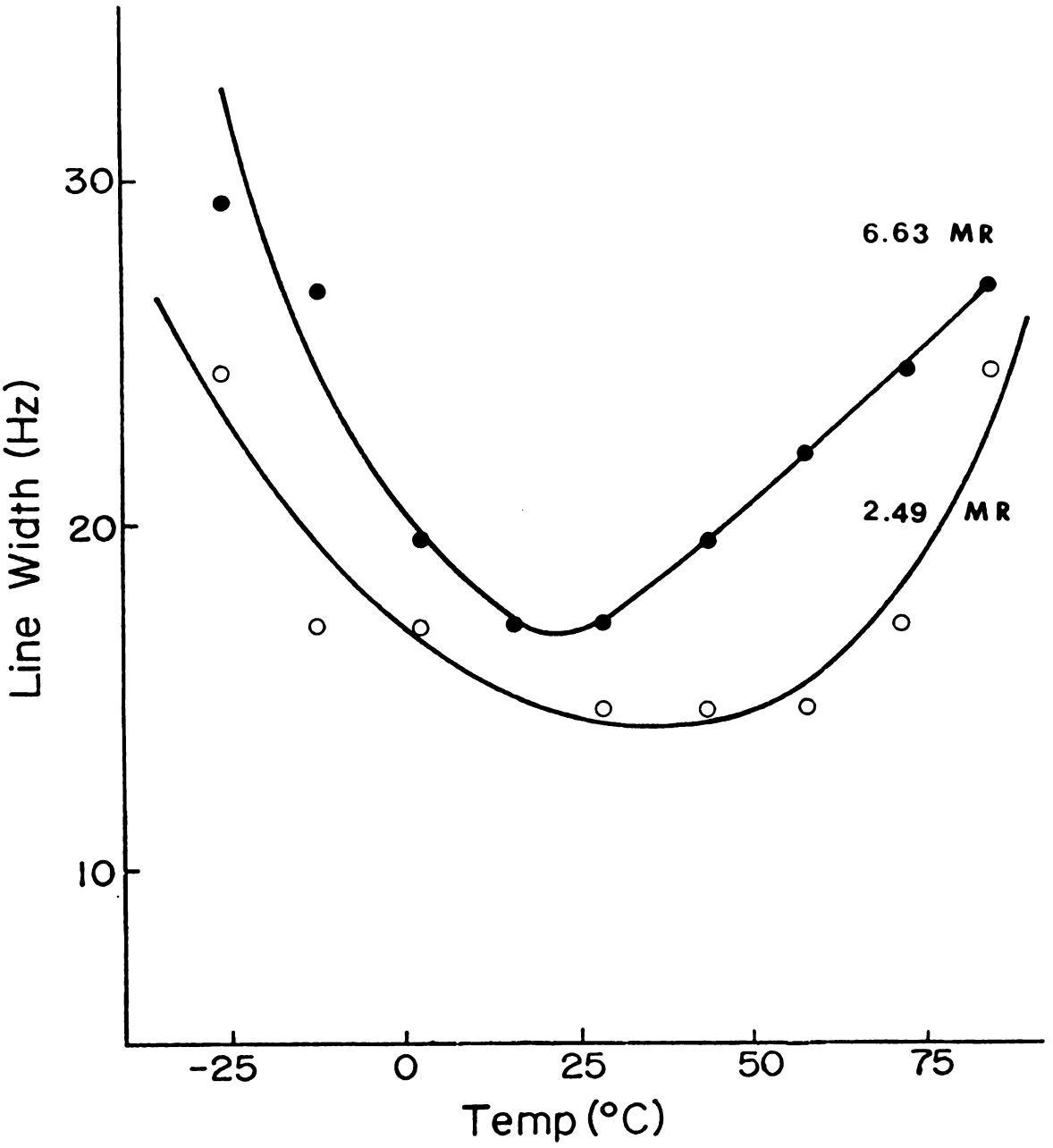

Figure 26. Temperature Dependence of the Uncorrected ^{133}Cs NMR Line Widths of $CsB\phi_4$- C211 Cryptates in Pyridine.
MR = [C211] /[Cs^+].

LITERATURE CITED

LITERATURE CITED

1. Y. M. Cahen, P. R. Handy, E. T. Roach and A. I. Popov, J. Phy. Chem., 79, 80 (1975).

2. E. G. Bloor and R. G. Kidd, Can. J. Chem., 46, 3425 (1968).

3. M. S. Greenberg, R. L. Bodner and A. I. Popov, J. Phy. Chem., 77, 2449 (1973).

4. G. E. Maciel, J. K. Hancock, L. F. Lafferty, P. A. Mueller and W. K. Musker, Inorg. Chem., 5, 554 (1966).

5. R. H. Erlich and A. I. Popov, J. Am. Chem. Soc., 93, 5620 (1971).

6. R. L. Bodner, M. S. Greenberg and A. I. Popov, Spectrosc, Lett., 5, 489 (1972).

7. Y. M. Cahen, J. L. Dye and A. I. Popov, J. Phy. Chem., 79, 1289 (1975).

8. T. L. James and J. H. Noggle, J. Am. Chem. Soc., 91, 3424 (1969).

9. P. G. Gertenbach and A. I. Popov, J. Am. Chem. Soc., 97, 4738 (1975).

10. J. P. Kintzinger and J. M. Lehn, J. Am. Chem. Soc., 96, 3313 (1974).

11. J. L. Dechter and J. I. Zink, J. Am. Chem.Soc., 98, 845 (1976).

12. E. G. Bloor and R. G. Kidd, Can. J. Chem., 50, 3926 (1972).

13. M. S. Greenberg and A. I. Popov, Spectrochim. Acta, 31A, 697 (1975).

14. A. I. Mishustin and Y. M. Kessler, J. Solution Chem., 4, 779 (1975).

15. W. Sahm and A. Schwenke, Z. Naturforsch., A29, 1754 (1974).

16. C. Deverell and R. E. Richards, Mol. Phys., 10, 551 (1966).

17. J. M. Crawford and R. P. H. Gasser, Trans. Faraday Soc., 63, 2758 (1967).

18. H. S. Gutowsky and B. R. McGarvey, Phys. Review, 91, 1423 (1953).

19. N. Bloembergen and P. P. Sorokin, Phys. Review, 110, 865 (1958).

20. R. Baron, J. Chem. Phys., 38, 173 (1963).

21. A. Carrington, F. Dravnicks and M. C. R. Symons, Mol. Phys., 3, 174 (1960).

22. O. Lutz, Z. Naturforsch., A22, 286 (1967).

23. J. Halliday, H. D. W. Hill and R. E. Richards, Chem. Commun., 219 (1969).

24. A. Loewenstein and M. Shporer, Chem. Commun., 214 (1968).

25. J. D. Hallidat, R. E. Richards and R. R. Sharp, Proc. Roy. Soc. London, A313, 45 (1969).

26. C. Hall, R. E. Richards and R. R. Sharp, Proc. Roy. Soc. London, A337, 297 (1974).

27. W. J. DeWitte, R. C. Schoening and A. I. Popov, Inorg. Nucl. Chem. Lett., 12, 251 (1976).

28. U. Mayer and V. Gutmann, Struct. Bonding (Berlin), 12, 113 (1972).

29. U. Mayer, V. Gutmann and W. Gerger, Monatshefte für Chemie, 106, 1235 (1975).

30. V. Gutmann and E. Wychera, Inorg. Nucl. Chem. Lett., 2, 257 (1966).

31. T. R. Griffiths and M. C. R. Symons, Mol. Phys., 3, 90 (1960).

32. J. C. Evans and G. Y.-S. Lo, J. Phy. Chem., 69, 3223 (1965).

33. K. Balasubrahmanyam and G. J. Janz, J. Am. Chem. Soc., 92, 4189 (1970).

34. R. C. Connick and R. E. Poulson, J. Phy. Chem., 62, 1002 (1958).

35. A. Carrington and T. Hines, J. Chem. Phys., 28, 727 (1958).

36. M. S. Greenberg, Ph.D. Thesis, Michigan State University, 1974.

37. B. W. Maxey and A. I. Popov, J. Am. Chem. Soc., 91, 20 (1969).

38. R. L. Kay, J. Am. Chem. Soc., 82, 2099 (1960).

39. R. L. Kay, B. J. Hales and G. P. Cunningham, J. Phy. Chem., 71, 3925 (1967).

40. S. Minc and L. Werblem, Electrochimica Acta, 7, 257 (1962).

41. C. Atlani and J-C. Justice, J. Solution Chem., 4, 955 (1975).

42. H. A. Berman and T. R. Stengle, J. Phy. Chem., 79, 1001 (1975).

43. T. L. Story, Jr. and A. J. Hebert, J. Chem. Phys., 64, 855 (1976).

44. A. Carrington, F. Dravnicks and M. C. R. Symons, Mol. Phys., 3, 174 (1960).

45. R. E. Richards and B. A. Yorke, Mol. Phys., 6, 289 (1963).

46. C. H. Langford and T. R. Stengle, J. Am. Chem. Soc., 91, 4014 (1969).

47. T. R. Stengle, Y-C. E. Pan and C. H. Langford, J. Am. Chem. Soc., 94, 9037 (1972).

48. C. Deverell and R. E. Richards, Mol. Phys., 16, 421 (1969).

49. D. C. Tosteson, Fed. Proc., 27, 1269 (1968).

50. R. M. Izatt, R. H. Rytting, D. P. Nelson, B. L. Haymore and J. J. Christensen, Science, 164, 443 (1969).

51. B. Dietrich, J. M. Lehn and J. P. Sauvage, Tetrahedron Lett., 2885 and 2889 (1969).

52. B. Dietrich, J. M. Lehn, J. P. Sauvage and J. Blanzat, Tetrahedron, 29, 1629 (1973).

53. J. M. Lehn, Struct. Bonding, 16, 1 (1973).

54. J. M. Ceraso and J. L. Dye, J. Org. Chem., 38, 1773 (1973).

55. D. Moras, B. Metz and R. Weiss, Acta Crystallogr., B29, 388 (1973).

56. Ibid, B29, 383 (1973).

57. D. Moras and R. Weiss, Acta Crystallogr., B29, 396 (1973).

58. Ibid, B29, 400 (1973).

59. J. M. Lehn and J. P. Sauvage, J. Am. Chem. Soc., 97, 6700 (1975).

60. B. Dietrich, J. M. Lehn and J. P. Sauvage, Chem. Commun., 15 (1973).

61. Y. M. Cahen, Ph.D. Thesis, Michigan State University, 1975.

62. J. M. Ceraso and J. L. Dye, J. Phy. Chem., 61, 1585 (1974).

63. F. J. Tehan, B. L. Barnett and J. L. Dye, J. Am. Chem. Soc., 96, 7203 (1974).

64. J. L. Dye, C. W. Andrews and S. E. Mathews, J. Phy. Chem., 79, 3065 (1975).

65. J. L. Dye, C. W. Andrews and J. M. Ceraso, J. Phys. Chem., 70, 3076 (1975).

66. J. S. Shih, private communication.

67. C. J. Pedersen, J. Am. Chem. Soc., 89, 7017 (1967).

68. Ibid, 92, 5226 (1970).

69. E. Mei, J. L. Dye and A. I. Popov, J. Am. Chem. Soc., 98, 1619 (1976).

70. J. M. Lehn, J. P. Sauvage and B. Dietrich, J. Am. Chem. Soc., 92, 2916 (1970).

71. E. Shchori, J. Jagur-Grodzinski, Z. Luz and M. Shporer, J. Am. Chem. Soc., 93, 7133 (1971).

72. E. Shchori, J. Jagur-Grodzinski and M. Shporer, J. Am. Chem. Soc., 95, 3842 (1973).

73. J. P. Kintzinger and J. M. Lehn, J. Am. Chem. Soc., 96, 3313 (1974).

74. J. M. Ceraso and J. L. Dye, J. Am. Chem. Soc., 95, 4432 (1973).

75. Y. M. Cahen, J. L. Dye and A. I. Popov, J. Phy. Chem., 79, 1292 (1975).

76. V. M. Loyola, R. G. Wilkins and R. Pizer, J. Am. Chem. Soc., 97, 7382 (1975).

77. E. Shchori, N. Nae and J. Jagur-Grodzinski, J. C. S. Dalton, 22, 2381 (1975).

78. S. Villermaux and J-J. Delpuech, Chem. Commun., 478 (1975).

79. S. Boileau, P. Hemery and J-C. Justice, J. Solution Chem., 4, 873 (1975).

80. B. Dietrich, J. M. Lehn and J. Simon, Angew. Chem., 13, 406 (1974).

81. J. M. Lehn, J. Simon and J. Wagner, Angew. Chem., 85, 622 (1973).

82. J. Cheney, J. M. Lehn, J. P. Sauvage and M. E. Stubbs, Chem. Commun., 1100 (1972).

83. S. M. Elinkova, Y. Y. Maksimov and E. Y. Orlova, Izv. Vyssh. Ucheb. Zaved., Khim. Khim. Teckhnol., 14, 176 (1971).

84. D. D. Traficante, J. A. Simms and M. Mulvay, J. Mag. Res., 15, 484 (1974).

85. D. A. Wright and M. T. Rogers, Rev. Sci. Instr., 44, 1189 (1973).

86. D. H. Live and S. I. Chan, Anal. Chem., 42, 791 (1970).

87. G. J. Templeman and A. L. Van Geet, J. Am. Chem. Soc., 94, 5578 (1972).

88. J. L. Dye and V. A. Nicely, J. Chem. Ed., 48, 443 (1971).

89. A. Saika and C. P. Slichter, J. Chem. Phys., 22, 26 (1954).

90. J. D. Memory, Quantum Theory of Magnetic Resonance Parameters, New York: McGraw-Hill Book Co., 1968, pp. 79-86.

91. R. F. Bacher, Atomic Energy States, New York: Greenwood Press, 1968.

92. A. D. Buckingham, T. Schaefer and W. G. Schneider, J. Chem. Phys., 32, 1227 (1960).

93. W. J. DeWitte, Ph.D. Thesis, Michigan State University, 1975.

94. J. M. Lehn and J. P. Sauvage, Chem. Commun., 440 (1971).

95. H. M. McConnell, J. Chem. Phys., 28, 430 (1958).

96. E. Mei, private communication.

97. Y. M. Cahen, J. L. Dye and A. I. Popov, Inorg. Nucl. Chem. Lett., 10, 899 (1974).